CIRRELT
Centre interuniversitaire de recherche
sur les réseaux d'entreprise, la logistique et le transport
Interuniversity Research Centre
on Enterprise Networks, Logistics and Transportation

Prepositioning Emergency Supplies to Support Disaster Relief: A Stochastic Programming Approach

Walid Klibi
Soumia Ichoua
Alain Martel

March 2013

CIRRELT-2013-19

Document de travail également publié par la Faculté des sciences de l'administration de l'Université Laval, sous le numéro FSA-2013-004.

Bureaux de Montréal :
Université de Montréal
C.P. 6128, succ. Centre-ville
Montréal (Québec)
Canada H3C 3J7
Téléphone : 514 343-7575
Télécopie : 514 343-7121

Bureaux de Québec :
Université Laval
2325, de la Terrasse, bureau 2642
Québec (Québec)
Canada G1V 0A6
Téléphone : 418 656-2073
Télécopie : 418 656-2624

www.cirrelt.ca

Prepositioning Emergency Supplies to Support Disaster Relief: A Stochastic Programming Approach

Walid Klibi[1,2,*], Soumia Ichoua[1,3], Alain Martel[1,4]

[1] Interuniversity Research Centre on Enterprise Networks, Logistics and Transportation (CIRRELT)

[2] Operation Management and Information Systems Department, BEM-Management School, 680 cours de la Libération, 33405 Talence Cedex, Bordeaux, France

[3] Department of Business Administration, Embry-Riddle Aeronautical University, 600 South Clyde Morris Blvd., Daytona Beach, FL 32114600, USA

[4] Department of Operations and Decision Systems, 2325, de la Terrasse, Université Laval, Québec, Canada G1V 0A6

Abstract. This paper studies the strategic problem of designing emergency supply networks to support disaster relief over a planning horizon. This problem addresses decisions on the location and number of distribution centers needed, their capacity, and the quantity of each emergency item to keep in stock in time. To tackle the problem, a scenario based approach is proposed involving three phases: disasters scenario generation, design generation and design evaluation. Disasters are modeled as stochastic processes and a Monte Carlo procedure is derived to generate plausible catastrophic scenarios. Based on this detailed representation of disasters, a multi-phase modeling framework is proposed to design the emergency supply network. The two-stage stochastic programming formulation proposed is solved using a sample average approximation method. This scenario based solution approach is tested with a case inspired from real-world data to generate plausible scenarios, to produce a set of alternative designs and then to evaluate them on a set of performance measures in order to select the best design.

Keywords. Humanitarian logistics, relief network design, risk modeling, multi-hazards, stochastic programming, Monte Carlo scenarios.

Acknowledgements. Financial support for this work was provided by the National Science Foundation (NSF) through grant number 0927129 (S. Ichoua). This support is gratefully acknowledged.

---

* Corresponding author: Walid.Klibi@cirrelt.ca

Dépôt légal – Bibliothèque et Archives nationales du Québec
Bibliothèque et Archives Canada, 2013

1. Introduction

In the last decade, the world has noticed an escalating trend in the number of natural disasters. In 2010, 385 natural disasters were reported worldwide killing more than 297,000 persons, affecting over 217 million others and causing US$ 123.9 billion in economic damages (Guha-Sapir et al., 2011). Despite the alarming effects of these disasters on global economy, mitigating their impacts on human lives remains the major concern. Hence, when a major disaster strikes, the challenge is to deliver the appropriate emergency supplies in sufficient quantities exactly when and where they are needed. Thus, the efficiency of logistics operations that account for 80% of relief operations (Van Wassenhove, 2006) is crucial in order to insure a good responsiveness when disasters occur. To ensure an adequate and timely response, humanitarian organizations managing relief aid in disaster-prone regions typically preposition different emergency supplies at some distribution centers (DCs) in these regions. Prepositioning decisions include the number and locations of the permanent DCs needed; their capacity and the quantity of each item they should hold. These decisions are constrained by budget limitations that restrict pre-disaster expenses dedicated to establishing DCs and holding inventories. Thus the challenge is to find a good trade-off between maximizing demand coverage and minimizing setup and operating costs. The literature on humanitarian logistics, including pre-disaster preparedness and post-disaster responsiveness, has grown in the past two decades (Atlay and Green (2006), Simpson and Hancock (2009) and Ichoua (2011)). However, there is still a lack of modeling and solution approaches that can efficiently address the challenging operating conditions of an emergency scene (i.e., making urgent decisions throughout the disaster lifecycle in a highly dynamic risky environment where information is scarce).

The contribution of this paper is threefold. First, to characterize potential threats, we propose a risk modeling approach based on time-space stochastic processes that builds on the general framework proposed in Klibi and Martel (2012). Hence, in addition to modeling disasters of multiple types, these multi-hazards unfold dynamically over time, leading to dynamic-stochastic scenarios. Each of these scenarios consists of a chronological list of multi-hazards characterized by an occurrence time as well as the impact on demand and availability of prepositioned supplies at DCs and at supply sources. Second, to account for the particularities of disaster evolution throughout its main stages (i.e., deployment, sustainment and recovery), a multi-phase modeling framework based on stochastic phase-dependent demands is proposed to tackle the prepositioning problem. Third, while most papers in the literature of humanitarian relief networks address two-echelon DC/Demand distribution systems, we propose a three-echelon system that also considers suppliers (i.e., pre-selected vulnerable vendors with limited resources and a backup source). The intent is to replicate real-life emergency settings as practiced for instance by Wal-

Mart response during Hurricane Katrina in 2005[1] or by Home depot contingency plans during Hurricane Gustav in 2008[2].

The remainder of the paper is organized as follows. Section 2 provides a non-exhaustive review of existing work related to pre-disaster preparedness. Section 3 describes the problem context. Section 4 presents the proposed risk modeling approach which depicts how multi-hazards unfold randomly in time over a planning horizon and in space over the geographical region under consideration. Section 5 presents the stochastic multi-phase mathematical program developed for the prepositioning problem. Section 6 describes the solution approach used to solve the prepositioning problem and to evaluate the performance of the relief network designs produced. Section 7 reports computational results obtained on a set of plausible scenarios inspired from real-world data. Finally, section 8 summarizes our findings and proposes future research avenues.

2. Literature Review

In the last two decades, the field of humanitarian logistics has gained increasing attention. Interesting survey papers on pre-disaster preparedness and post-disaster responsiveness include Atlay and Green (2006), Simpson and Hancock (2009) and Ichoua (2011). This section solely presents a non-exhaustive review of existing work related to pre-disaster preparedness. Many papers within this research line are dedicated to pre-positioning problems formulated as variants of facility location models (Daskin, 1995 and Snyder, 2006). In the following, the literature on pre-disaster preparedness is classified in two major categories, depending on whether the modeling approach is deterministic or stochastic. Within each category, a classification is made based on the type of disruptions modeled: demand, capacity (complete/partial loss of pre-positioned supplies) and transportation network (lane perturbations) disruptions. It is worth noticing that complete loss of capacity or facility failure has been relatively well studied compared to partial loss of capacity. Snyder et al. (2006) present a set of facility location models for designing reliable/fortified networks to facility failures.

2.1 Deterministic Models

Papers that belong to this category either assume that problem inputs such as impacted populations demand size and state of the transportation networks are all known with certainty or use single-point estimates for these inputs. In the former case, temporary facilities must be located at the beginning of the disaster and may need to be relocated at different time periods during the response duration. The problem is operational rather than strategic. It is thus assumed that necessary information can be obtained and updated each time location-relocation decisions need to be made. Papers that use deterministic inputs often address disaster impact on demand only

[1] Source: Wal-Mart at Forefront of Hurricane Relief (The Washington Post, 2005/09/05)
[2] Source: money.cnn.com (Home Depot's hurricane plan - Fortune , 2010)

(Dekle et al. (2005), Tzeng et al. (2007), and Halper and Raghavan (2011)). In Nolz et al. (2011), transportation network disruption is also addressed. In the case of single-point estimates, historic data are used to forecast expected values of the inputs (Iakovou et al. (1996) and Akkihal (2006)) or input values corresponding to the worst or best case (Gormez et al. (2011)). These values are then used as parameters in deterministic models.

When establishing temporary facilities to respond to a disaster, it is reasonable to use deterministic values for the problem inputs, provided a timely accessibility to information needed. The latter is affordable nowadays with the advances in information technology. However, when addressing the strategic decision of establishing permanent facilities to prepare for future disasters over a long time planning horizon, problem information is uncertain due to the time lag. Thus, the use of single point estimates is likely to lead to poor network performance. Stochastic modeling approaches are aimed at overcoming this weakness.

2.2 Stochastic Models

This line of research has sought to develop robust modeling and solution approaches that account for the randomness in some problem inputs such as demand and availability of transportation. For relatively simple cases (e.g. a single facility or demand point), continuous probability distributions are used. When more realistic cases are considered, scenario-based approaches are favored to limit the possible outcomes to a finite set of plausible futures. In the following, we briefly review some of the work that belongs to these two categories.

Modeling Demand Disruption Only

Continuous probability distributions were used in Lodree and Taskin (2008a,b) to address inventory control problems aimed at finding optimal level of emergency supplies to preposition at a known facility. Murali et al. (2011) assume that demand of medicine follows a log-normal distribution when addressing the problem of prepositioning medicine in capacitated facilities. They propose a chance constrained programming model which maximizes coverage while guarantying an upper-bound on the probability of violating demand constraints.

Chang et al. (2007) examine the problem of prepositioning rescue resources in preparation for floods. They propose two stochastic programming models to minimize total expected set up, transportation and equipment costs. Their models are solved using a sample average approximation schema. Duran et al. (2011) also use a scenario-based approach for a similar problem. It is assumed that demand for relief supplies can be met from prepositioned quantities and suppliers. The proposed mixed integer programming model minimizes the expected average response time assuming a limit on total inventory allowed and on the number of warehouses to open. A scenario-based approach is also used in Balcik and Beamon (2008) who propose a variant of the maximal covering location model with objective to maximize covered demand under pre-disaster and

post-disaster budget constraints. However, in their model scenarios involve a single event (i.e., a single demand location and amount).

Finally, a scenario-based approach was also applied for designing a global supply network to support the humanitarian assistance, peacekeeping and peace enforcement missions of the Canadian Armed Forces in Martel et al., (2012). A scenario generation procedure is proposed to generate worldwide disasters and conflicts over a planning horizon, to determine if these give rise to a mission and, if so, to specify product demands and returns at specific locations during the mission deployment, sustainment and redeployment phases.

Modeling Demand and Capacity/Transportation Network Disruption

In Ukkusuri and Yushimoto (2008), the problem of pre-positioning supplies is modeled as a location-routing problem where some pre-selected transportation links have a known probability of failure. The objective is to maximize the probability to reach all demand points. The proposed integer programming model integrates a procedure for finding the most reliable paths. A continuous probability distribution is also used in Campbell and Jones (2011) to model demand when considering the problem of locating supply points and deciding on their levels of inventory given that each of these has a known probability of being destroyed. The authors determine the optimal stocking quantity and the total expected costs associated with delivering to a demand point from a single supply point. The results are then used in a heuristic which address the case of multiple demand and supply points. However, it is assumed that each demand point is served by a single facility.

Jia et al. (2007) develop a scenario-based approach to solve different variants of facility location models for the prepositioning of supplies in large-scale emergencies. The models use a set of discrete scenarios to represent the likelihood that a certain emergency situation affects a given demand point. The models also account for the reduction in service capability of a facility under an emergency scenario. However, in their illustrative example, the authors do not consider facility disruptions. Mete and Zabinsky (2010) examine the problem of prepositioning medical supplies under demand and transportation disruptions. Six scenarios are used to represent different demand and travel time realizations based on earthquake data in the Seattle area. The authors propose a two-stage stochastic model which integrates location and inventory decisions. The objective is to minimize the expected sum of fixed and transportation costs along with a penalty of unsatisfied demand.

Rawls and Turnquist (2010) model a similar problem as a two-stage stochastic program, solved using a heuristic which combines the L-shaped method and Lagrangian relaxation. They consider demand, transportation and capacity disruptions. Historical data from a sample of fifteen hurricanes in the southeastern US are used to generate 51 probabilistic scenarios. Rawls and

Turnquist (2011), extend the model to include service quality constraints using the notion of reliable sets introduced in Daskin et al. (1997). This model is extended further in Rawls and Turnquist (2012) to account for time-dependent static demand over the deployment phase which is partitioned into four time periods. The model also uses time-dependent capacities on flows between origins and destinations to account for transportation link damages. However, capacities on flows are not implemented in the reported experiments.

The literature review reveals that despite the increased interest in scenario-based approaches for humanitarian relief network design, to the best of our knowledge all existing models are based on static scenarios that overlook the dynamic-stochastic nature of multi-hazard occurrences. When compared to generic extreme events modeling frameworks available in the literature (Grossi and Kunreuther, 2005; Banks, 2006), it appears that the hazards characterization in current relief network design models is too simplistic. In addition, these models account for the deployment phase only of the disaster relief cycle, therefore ignoring the particular needs of subsequent phases (sustainment, recovery and redeployment). Moreover, emergency distribution networks are often modeled as two-echelon DC/Demand distribution systems that ignore contracted vendors and backup sources that are major players in real-life humanitarian supply chains. Their inclusion at the design level is crucial to adequately anticipate the challenging problem of efficient coordination during relief operations (Van Wassenhove, 2006). This paper is aimed at overcoming these drawbacks.

3. Problem Context

We consider a geographical region which is prone to multiple natural disasters over a given discrete time horizon. These disasters have different severity levels and are of different categories e.g. floods, hurricanes, earthquakes, etc. They may strike random zones within the region therefore resulting in stochastic demands of different types of emergency supplies (referred to as *items* in this text). Some lifesaving items such as packaged food, water, ice and tarps are required for all disasters. These items can be partitioned into two sets: consumable items and durable assets. Each item type is characterized by a target response time. Prior to a disaster onset, a humanitarian organization which manages relief aid in the geographical region typically preposition different items at some DCs in that region. The intent is to ensure an adequate and timely response. To help achieving this goal, each zone jurisdiction also identifies a set of Points of Distribution (PODs) from where items will be directly issued to populations in need. A population-based PODs dispersion over the disaster-prone area is provided to shape adequately the demand zone characteristics in terms of needs, distance coverage and delays.

Prepositioning decisions include the number and locations of DCs needed; their capacity and the quantity of each item they should hold. These decisions are constrained by budget limitations

that restrict pre-disaster expenses dedicated to establishing DCs and holding inventories. Prepositioned items are used afterward to respond to disasters that may unfold within the planning horizon. During a given disaster, contractual transportation services are used to conduct daily distribution of items to affected populations for the disaster response duration. This period can typically be divided into four phases: deployment, sustainment, recovery and redeployment. While durable assets need to be delivered to PODs only during the deployment phase, consumable items must be shipped to these PODs during the deployment, sustainment and recovery phases. Deployed reusable items are returned to the DCs during the redeployment phase.

The deployment is characterized by a chaotic setting where demand surge is high and DCs cannot be replenished. The duration of this hectic status corresponds to the deployment lead time (i.e., the time it takes to restore the infrastructure needed to resupply the DCs). Quick relief aid must be provided to affected populations using existing items at DCs. When prepositioned supplies are depleted, demand may be satisfied from vendors that have been pre-selected on the basis of best value bids. In this bidding process, vendors specify their proposed price for each item, as well as the maximum quantity they can provide within pre-established target times. Pre-negotiated contracts are then awarded to vendors that meet the best combination of price, availability of stock and timely delivery. A backup source may also be used as last recourse in case supplies acquired from contract vendors are not sufficient to satisfy demand in a timely manner. This backup source may represent federal authorities, military support, regional collaborations, etc… To better cope with high time pressure which is inherent to the deployment phase, a service-based objective function is needed.

The sustainment phase lasts generally longer than the deployment and is characterized by a stationary demand and the availability of functional DC resupply lines. Thus, vendors and the backup source are able to replenish DCs up to their desired stock levels. During this less chaotic phase, the satisfaction of the demand at the PODs is allowed solely from the DCs and contract vendors. During the recovery phase, demand for relief efforts decreases gradually as the infrastructure and essential services at affected zones recuperate. Operations similar to those conducted during sustainment must be performed to satisfy this gradually decreasing demand. During both the sustainment and recovery phases, the objective is to minimize total procurement and transportation costs. The redeployment phase starts when relief efforts are completed and finishes when all assets and unused items are moved back to DCs.

It is worth noticing that humanitarian organizations are generally responsible for operations in the four phases. However, since redeployment operations take place in a stable environment with no time pressure, we do not consider this phase explicitly. The underlying assumption is that relief operations during the time to recovery are more critical. On the other hand, we assume that disasters are independent and therefore, since the deployment phase is relatively short, it is

unlikely that two disaster deployments would have to be made from a given DC during a deployment lead time. Hence, prepositioned quantities are sufficient to ensure an adequate responsiveness. **Figure 1** illustrates the type of relief distribution network considered in this paper. In this figure, the indexes and sets $p \in P, i \in I, v \in V$ and $j \in J$ denote items, PODs, vendors ($v = 0$ denotes the backup source) and DCs, respectively. The set K_j represents possible capacity configurations for DC j. The network consists of three types of nodes (supply sources, DCs and PODs) and three types of flows (deployment, sustainment/recovery and resupply).

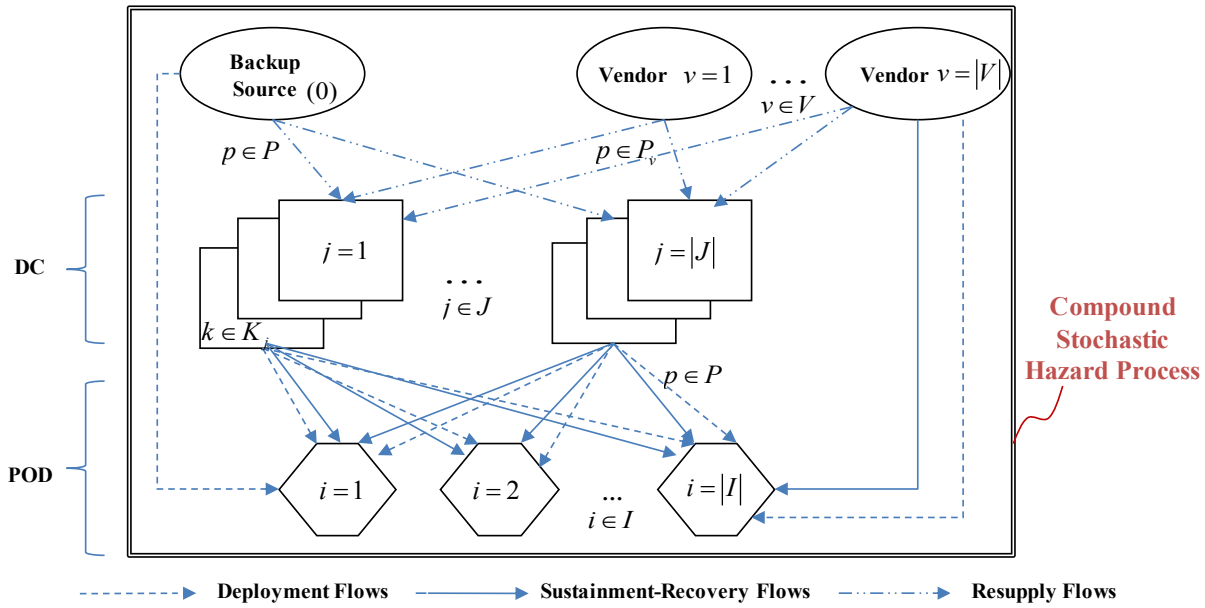

Figure 1: The Relief Distribution Network

When a disaster hits a given zone, its impact on the relief network performance depends on four vulnerability sources, namely vendors, DCs, PODs and transportation lanes. It is assumed that the back-up source is always available. Disaster impact associated to the four vulnerability sources can be represented by stochastic perturbations that distress the quantity of supplies that vendors can provide, capacity levels at DCs, demand levels at PODs and/or travel times on transportation lanes. Furthermore, disaster impact on a given hit zone varies within its life cycle. Hence, during the deployment phase, the storage capacity of a hit DC or vendor decreases and remains stagnant during the sustainment phase before it starts ramping up during the recovery phase. This could lead during the planning horizon to the temporary unavailability of a subset of DCs and vendors for a given hazard. Conversely, demand at a hit POD increases during the deployment stage till it reaches a maximum that is maintained during the sustainment phase. This amount then decreases during the recovery phase. On the other hand, travel time perturbations are likely to be more pronounced during the deployment phase which is generally more chaotic. Therefore, a multi-phase formulation based on stochastic phase-dependent demands, capacities and travel times judiciously represents a disaster scene. Addressing the problem of preposition-

ing emergency supplies accurately requires a judicious modeling of the disaster process. To this end, the next section presents a risk modeling approach which builds on the general framework proposed in Klibi and Martel (2012).

4. Modeling the Disaster Process

The proposed risk modeling approach is based on a compound stochastic process which represents how hazards unfold randomly in time over the planning horizon, and in space over the geographical region under consideration. Given a partition of the region into a set of zones, the proposed risk modeling approach depicts the hazard process in two steps. The first step characterizes hazard attributes including occurrence time, intensity and severity. The second step models hazard impact on response duration, items demand as well as ability of DCs and vendors to supply items needed. It is assumed that transportation lanes are not directly disrupted and that DCs and vendors disruption is sufficient to capture the perturbation of deliveries in terms of available inventories and transportation. The resulting stochastic processes are used to generate a set of equiprobable scenarios using Monte-Carlo methods. In the following, the risk modeling approach and the Monte-Carlo procedure are described in details.

1.1. Disaster Attributes

We consider a geographical region prone to disasters in time. These disasters are grouped into generic meta-events, called multi-hazards (Scawthorn et al., 2006), based on their similar impact from the perspective of the relief network. Multi-hazards that threaten the region have similar characteristics that depend on the region geological and meteorological features. These characteristics, including intensity, severity and occurrence frequency, are determined from historical data and expert-based catastrophic risk assessments. We assume that hazards occur in the region at the beginning of discrete time periods corresponding to days, within a long planning horizon *T*. The resulting multi-hazard arrival process is characterized in terms of random inter-arrival times with probability distribution $F_\lambda(.)$, where λ represents the inter-arrival time between two consecutive multi-hazards. Using historical hazards data, an exponential distribution with estimated mean $\bar{\lambda}$ is generally the best fit for multi-hazards inter-arrival times (Banks, 2006).

Additionally, the intensity β^h of an occurring hazard h characterizes its physical impact. Hazard intensity β^h is a random variable which follows a given probability distribution $F_\beta(.)$. Moreover, hazard severity can be measured by the magnitude of relief interventions that hazard h triggers. The extent of these interventions in terms of emergency items needed and response duration depends on the hazard physical impact. Thus hazard severity is a random variable correlated to β^h. Though hazard h presents a threat to the entire region, its severity and impact can vary from one part of the region to another. To capture this variability, the region is partitioned

into a set of zones $z \in Z$. We assume that zones $z \in Z$ uniformly inherit the region hazard intensity while hazard severity is generally zone-dependent. Accordingly, hazard severity at zone z is a random variable denoted ρ_z^h which follows a given probability distribution $F_{\rho_z(\beta^h)}(.)$. In this paper, hazard severity ρ_z^h is modeled as a fraction used to determine the number of habitants who are likely to stay in zone z following hazard h (e.g. elderly people, homeless, financially challenged families/individuals, etc…).

Finally, to account for future environmental changes, a set of probabilistic evolutionary trends $\kappa \in \mathrm{K}$ is used. Each trend κ occurs with a given probability p_κ, $\kappa \in \mathrm{K}$. We assume that these trends have an impact on the mean time between multi-hazards, but not on their severity. Therefore, under evolutionary trend κ, a function $g_\kappa(.)$ is used to superimpose a time pattern on the historical mean time between hazards $\bar{\lambda}$ estimated at the beginning of the planning horizon T. Thus, under trend κ, the time between a hazard occurring at the beginning of period $t \in T$ and a subsequent one is an exponentially distributed random variable with mean $\bar{\lambda}_{t\kappa} = g_\kappa(\bar{\lambda}, t)$.

1.2. Disaster Impact

When a multi-hazard h strikes at the beginning of time period $t \in T$, its impact on the region is zone-dependent. Thus, a compound propagation process is used to determine the subset $Z^h \subset Z$ of zones impacted by hazard h, and its *centroid* zone, i.e. the main affected zone. The probability that zone z is the multi-hazard centroid zone when there is a hit is denoted $\pi_z, z \in Z$. Since multi-hazard h is likely to propagate to other zones in the vicinity of its centroid, a set of adjacent zones $z' \in Z$ are added to Z^h using conditional propagation probabilities denoted $\alpha_{z'|z}, z, z' \in Z$. Probabilities $\pi_z, z \in Z$ and $\alpha_{z'|z}, z, z' \in Z$ depend on the granularity of the zones defined. They are estimated using hazard frequencies derived from historical data that are collected over a time interval. These probabilities are calculated as follows:

$$\pi_z = n_z \Big/ \sum_{z \in Z} n_z \,, z \in Z \quad \text{and} \quad \alpha_{z'|z} = \frac{n_{z'|z}}{n_z} \,, z, z' \in Z \,,$$

where n_z denotes the number of hazards recorded for zone z over the time interval considered, and $n_{z'|z}$ is the number of times zone z' was affected when zone z was hit. Multi-hazard h impacts affect zones $z \in Z^h$ as follows:

- A relief response is needed in all zones $z \in Z^h$ for the incident duration.
- Demand of different items occurs in each zone $z \in Z^h$.
- DCs located in zones $z \in Z^h$ become unavailable.
- Supplies become inaccessible from vendors located in zones $z \in Z^h$.

When a multi-hazard h strikes, all zones $z \in Z^h$ are assumed to have the same time to recovery θ^h. The latter is a random variable correlated to hazard intensity β^h, therefore following a probability distribution $F_{\theta(\beta^h)}(.)$. Since prepositioning of emergency supplies deals with strategic planning rather than daily operations, the time to recovery θ^h is partitioned into three major phases: deployment (denoted *D*), sustainment (denoted *S*) and recovery (denoted *R*). The intent is to capture the particular needs of each phase while avoiding operational details that might be useless given the highly dynamic-stochastic nature of a disaster scene. The three phases were discussed in details in section 3. The duration of each phase is denoted by $\theta^{h\tau}, \tau = D, S, R$. The deployment phase duration θ^{hD} is generally short and is assumed to be fixed for all hazards. Thus, it will hereafter be denoted θ^D. When the time to recovery is longer than the deployment period, a sustainment phase is subsequently observed, followed by a recovery phase. The latter is assumed to last a fraction $\varphi \in [0,1]$ of the sustainment duration. Thus, for a given multi-hazard *h*, the sustainment and recovery phase durations are given by:

$$\theta^{hS} = \left\lfloor \frac{1}{1+\varphi} max(0,\ \theta^h - \theta^D) \right\rfloor \text{ and } \theta^{hR} = \lceil \varphi \theta^{hS} \rceil$$

On the other hand, when a multi-hazard *h* hits the region under consideration, a stochastic time and zone dependent demand for items $p \epsilon P$ arises in affected zones $z \in Z^h$. Let $d_{zpt}^{h\tau}$ be the demand for item $p \epsilon P$ in zone $z \in Z^h$ for period *t* within phase τ. This demand depends on hazard severity ρ_z^h, the population size of zone z which is known, and the daily need per habitant for product *p* in period *t* of phase τ. The latter is a random variable denoted ξ_{pt}^{τ} which follows a given probability distribution $F_{\xi_{pt}}(.)$. To ensure a timely relief, each zone $z \in Z^h$ is supported by a set of PODs $i \in I_z$ from where emergency items are directly issued to the population. The zone portion covered by each POD is predetermined by experts based on zip code aggregation or population density, and the population v_i served by POD $i \in I_z$ is thus defined. Consequently, for a given multi-hazard *h*, the demand of POD *i* for product *p* in period *t* within phase τ is a random variable, given by $d_{ipt}^{h\tau}$ and is correlated to random variable $\rho_{z(i)}^h$ with the following relation $d_{ipt}^{h\tau} = \rho_{z(i)}^h v_i \xi_{pt}^{\tau}$, where *z*(*i*) denotes the zone containing POD *i*.

Daily demand during the deployment phase is erratic and therefore, it is hard to estimate its probability distribution. Thus, the deployment phase is considered as a single period of length θ^D for which total demand of item $p \epsilon P$ at POD *i* is estimated as follows:

$$d_{ip}^{hD} = \theta^D \rho_{z(i)}^h v_i \bar{\xi}_p$$

Where $\bar{\xi}_p$ is an estimate of average daily need per habitant for product $p \epsilon P$.

Conversely, daily demand for consumable items during the sustainment phase is fairly stable. Let P^C be the subset of consumable items in *P*. When $\{\xi_{pt}^S\}$ is a stationary stochastic process with an estimated mean $\bar{\xi}_p$, $\{d_{ipt}^{hS}\}, p \in P^C$, is also a stationary process. Therefore it is rea-

sonable to assume that for every day t within phase S, d_{ipt}^{hS} follows a Normal distribution with mean μ_{ip}^{hS} and standard deviation σ_{ip}^{hS} given by:

$$\mu_{ip}^{hS} = \rho_{z(i)}^{h} v_i \bar{\xi}_p, \qquad \sigma_{ip}^{hS} = CV_p \mu_{ip}^{hS}$$

where CV_p is the coefficient of variation of the demand for product $p \in P^C$.

Furthermore, daily demand for relief items decreases during the recovery phase R as the infrastructure at affected zones gets restored. To reflect this trend, given hazard h starting date η^h, the average of the Normal demand of product $p \in P^C$ for day t of the recovery phase is calculated as follows:

$$\mu_{ipt}^{hR} = \mu_{ip}^{hS} - \mu_{ip}^{hS} \frac{t}{\eta^h + \theta^h}, i \in I_z, p \in P^C$$

Hence, starting from a fraction of the sustainment average daily demand μ_{ip}^{hS} at the beginning of the recovery phase, μ_{ipt}^{hR} decreases till it reaches zero at the end of incident duration θ^h. The standard deviation is given by $\sigma_{ip}^{hR} = CV_p \mu_{ip}^{hR}$, as for the sustainment phase. **Figure 2** illustrates the resulting stochastic processes which describes demand patterns for a given item p throughout the planning horizon.

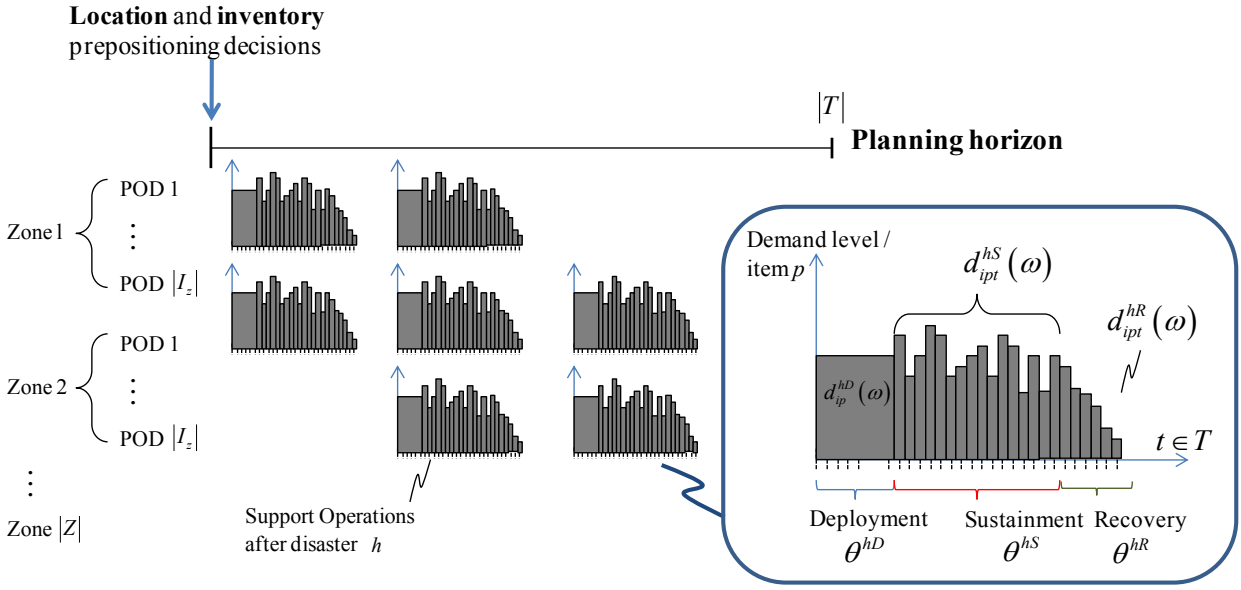

Figure 2- Demand Pattern for an Item p During the Planning Horizon

Finally, during the incident duration θ^h, the set J_z of DCs and the set V_z of vendors located in an affected zone $z \in Z^h$ could be hit by hazard h and therefore become unavailable. Let $z(j)$ and $z(v)$ denote the hazard zone enclosing DC j and vendor v, respectively. Conditional attenuation probabilities $\alpha_{j|z(j)}$ and $\alpha_{v|z(v)}$ are used to determine impacted DCs J^h and vendors V^h for a given hazard h within the affected zones set Z^h, respectively. These probabilities depend on the granularity of the zones defined and can be estimated using historical data and experts' assessment of facility exposure. Hereafter, J^h and V^h respectively denote the set of DCs and ven-

dors that are available during hazard h. Given the set V_p of vendors that can provide item $p \in P$, the subset V_p^h of available vendors for item p is derived as follows: $V_p^h = V^h \cap V_p$. We recall that disasters are assumed to be independent and therefore DC capacities and available quantities at vendors are fully restored before another multi-hazard hits.

1.3. Monte-Carlo Procedure

The Monte-Carlo procedure used to generate a disaster scenario ω is summarized in **Figure 3**. In this procedure, u denotes a uniformly distributed pseudo random number generated in the interval [0, 1], and $^{-1}(.)$ the inverse of the standardized Normal distribution. After selecting an evolutionary path, the procedure creates a chronological hazard list $\mathrm{H}(\omega)$. For each multi-hazard $h \in \mathrm{H}(\omega)$, the starting date η^h and the intensity β^h are computed. Then, the procedure generates multi-hazard response duration θ^h along with phase durations $\theta^{h\tau}, \tau = S, R$. Subsequently, the set Z^h of affected zones is determined and for each zone $z \in Z^h$ hazard severity ρ_z^h is generated. Afterwards, for each pre-identified POD $i \in I_z$ and for each item $p \in P$, the procedure generates the total deployment demand d_{ip}^{hD}. It also produces the daily demands $(d_{ipt}^{h\tau})_{\tau=S,R}$ for consumable items during the sustainment and recovery phases. Then, the sets of available DCs and vendors are identified. Finally, aggregated demands $(d_{ip}^{h\tau})_{\tau=S,R}$ over these two phases are derived and added to obtain total demand over the combined sustainment-recovery (*SR*) phase.

1) Select an evolutionary path κ randomly using p_κ, $\kappa \in \mathrm{K}$
2) Generate a chronological hazard list $\mathrm{H}(\omega)$:
   $\mathrm{H}(\omega) \equiv \varnothing$; $t = 0$
   While $t \leq |T|$, do:
      2.1) Calculate $\bar{\lambda}_{t\kappa} = g_\kappa(\bar{\lambda}, t)$ and compute the next hazard *h* arrival time $t = t + F_\lambda^{-1}(u)$, then set $\eta^h = \lceil t \rceil$
      2.2) Compute the hazard intensity $\beta^h = F_\beta^{-1}(u)$
      2.3) Insert hazard h with attributes (η^h, β^h) chronologically into the list $\mathrm{H}(\omega)$
   End While
3) Generate hazards severity and impacts:
   For all h in $\mathrm{H}(\omega)$, do:
      3.1) Generate hazard response duration and derive phase durations:
         Compute $\theta^h = F_{\theta(\beta^h)}^{-1}(u)$ and calculate $\theta^{h\tau}, \tau = S, R$ given θ^D
      3.2) Generate hazard locations, hazard severity at these locations and demands at their PODs:
         $Z^h \equiv \varnothing$, $J^h \equiv \varnothing$ and $V^h \equiv \varnothing$
         i) Select the hazard centroid zone $z = z_k \left| \sum_{j \leq k} \pi_{z_j} < u \leq \sum_{j < k+1} \pi_{z_j}, z_k \in Z \right.$ and update $Z^h = Z^h \cup \{z\}$
         ii) Construct the hazard zone propagation set:
            For all $z' \in Z / \{z\}$ do: If $(u \leq \alpha_{z'|z})$ then $Z^h = Z^h \cup \{z'\}$
         iii) For all $z \in Z^h$ do: generate $\rho_z^h = F_{\rho_z(\beta^h)}^{-1}(u)$

iv) Generate POD's daily deployment demand:

For all $z \in Z^h$, $i \in I_z$, $p \in P$ do: $d_{ip}^{hD} = \theta^D \rho_{z(i)}^h v_i \overline{\xi_p}$

v) Generate POD's daily sustainment and recovery demand:

For all $z \in Z^h$, $i \in I_z$, $p \in P^C$ do:

a) Compute $\mu_{ip}^{hS} = v_i \rho_{z(i)}^h \overline{\xi_p}$, $\sigma_{ip}^{hS} = \mathrm{CV}_p \mu_{ip}^{hS}$

and generate the daily sustainment demands:

$d_{ipt}^{hS} = \mu_{ip}^{hS} + {}^{-1}(u)\, \sigma_{ip}^{hS}$, $t = \eta^h + \theta^D, \ldots, \eta^h + \theta^D + \theta^{hS}$

b) Compute $\mu_{ipt}^{hR} = \mu_{ip}^{hS} - \mu_{ip}^{hS} \frac{t}{\eta^h + \theta^h}$, $\sigma_{ipt}^{hR} = CV_p \mu_{ipt}^{hR}$

and generate the daily recovery demands:

$d_{ipt}^{hR} = \mu_{ip}^{hR} + {}^{-1}(u)\, \sigma_{ip}^{hR}$, $t = \eta^h + \theta^D + \theta^{hS}, \ldots, \eta^h + \theta^h$

End For

vi) Identify available DCs and vendors:

For all $z \in Z^h, j \in J_z$: If $(u \le \alpha_{j|z(j)})$ then $J^h = J^h \cup \{j\}$

For all $z \in Z^h, v \in V_z$: If $(u \le \alpha_{v|z(v)})$ then $V^h = V^h \cup \{v\}$

End For

4) Aggregate demands over phases S and R:

For all $p \in P^C, i \in I_z, z \in Z^h$, $h \in \mathrm{H}(\omega)$

$d_{ip}^{hSR} = \sum_{\eta^h + \theta^D \le t \le \eta^h + \theta^D + \theta^{hS} - 1} d_{ipt}^{hS} + \sum_{\eta^h + \theta^D + \theta^{hS} \le t \le \eta^h + \theta^h - 1} d_{ipt}^{hR}$

End For

Figure 3- Monte Carlo Procedure for Scenario ω

5. Modeling the Prepositioning Problem

Prior to a hazard onset, emergency items must be prepositioned at some DCs to ensure an adequate and timely response. Prepositioning decisions include the number and locations of DCs needed; their capacity and the quantity of each emergency item they will hold. DC locations are chosen among a set J of pre-selected sites. Sites pre-selection is based on several criteria including political priorities, risk levels, proximity of highways, etc… Moreover, a set of feasible configurations K_j is associated to each DC j and each configuration $k \in K_j$ is characterized by a fixed usage cost f_{jk} and a capacity a_k (expressed in available space volume). A parameter o_p is used to convert the available quantity of item p into required space. Prepositioning decisions are constrained by a budget limit b which restricts pre-disaster expenses dedicated to establishing DCs and holding inventories. A holding cost e_{jp} is incurred for each unit of item p held in inventory at DC j. It is worth noticing that the budget limit b as well as the costs f_{jk} and e_{jp} are assumed to cover the entire planning horizon.

Prepositioning emergency supplies is a strategic decision aimed at designing the relief distribution network before a potential hazard strikes. The designed distribution network is used later to respond to hazards that may unfold within the planning horizon. This involves conducting daily operations aimed at delivering emergency supplies to affected populations and resupplying DCs for hazard durations. Hence, design decisions have a significant impact on daily re-

lief operations. Therefore, anticipating the impact of prepositioning decisions on emergency supplies daily distribution is essential to the enhancement of relief efforts. This anticipation represents operational decisions that optimize an estimate of some operational objective function under the approximate operational information available when design decisions are made. This leads to a two-stage stochastic programming model where the first stage addresses strategic design decisions while the second stage tackles operational decisions triggered by a hazard occurring within the planning horizon. The proposed model is presented below.

First Stage (strategic decisions)

As shown in section 4, hazards unfold over the planning horizon according to complex compound stochastic processes. Thus, a set $\Omega = \{\omega\}$ of probabilistic scenarios is used to compute total expected (anticipated) second stage value over the planning horizon. This expected value, denoted $\mathbf{E}\left(\mathrm{V}\left(\mathbf{X},\mathbf{Q}\right)\right)$, also depend on the strategic prepositioning decisions $\left(\mathbf{X},\mathbf{Q}\right)$ made, **X** and **Q** being vectors of the decision variables

$$X_{jk} = \begin{cases} 1, & \text{if } DC\ j \text{ is opened with configuration } k \in K_j \\ 0, & \text{otherwise (i.e., } DC\ j \text{ is closed)} \end{cases}$$

Q_{jp}: Quantity of item p to be held at DC j

and it is given by the expression $\mathbf{E}\left(\mathrm{V}\left(\mathbf{X},\mathbf{Q}\right)\right) = \sum_{\omega\in\Omega} p\left(\omega\right)\mathrm{V}\left(\mathbf{X},\mathbf{Q},\omega\right)$, where $p\left(\omega\right)$ is the probability of occurrence of scenario ω, and $\mathrm{V}\left(\mathbf{X},\mathbf{Q},\omega\right)$ is the optimal second stage value under scenario ω and prepositioning decisions $\left(\mathbf{X},\mathbf{Q}\right)$. Since a scenario $\omega \in \Omega$ is a set of plausible hazards $h \in \mathrm{H}(\omega)$, $\mathrm{V}\left(\mathbf{X},\mathbf{Q},\omega\right) = \sum_{h\in\mathrm{H}(\omega)} \mathrm{V}\left(\mathbf{X},\mathbf{Q},h\right)$, where $\mathrm{V}\left(\mathbf{X},\mathbf{Q},h\right)$ is the optimal second stage value under hazard $h \in \mathrm{H}(\omega)$ and decisions $\left(\mathbf{X},\mathbf{Q}\right)$. Consequently, the optimal value $\mathbf{E}\left(\mathrm{V}\left(\mathbf{X}^*,\mathbf{Q}^*\right)\right)$ is obtained by solving the following mathematical program:

$$\mathbf{E}\left(\mathrm{V}\left(\mathbf{X}^*,\mathbf{Q}^*\right)\right) = \mathrm{Min}_{\mathbf{X},\mathbf{Q}}\ \mathbf{E}\left(\mathrm{V}\left(\mathbf{X},\mathbf{Q}\right)\right) = \sum_{\omega\in\Omega} p(\omega) \sum_{h\in\mathrm{H}(\omega)} \mathrm{V}\left(\mathbf{X},\mathbf{Q},h\right) \tag{1}$$

subject to

$$\sum_{j\in J}\left(\sum_{k\in K_j} f_{jk}X_{jk} + \sum_{p\in P} e_{jp}Q_{jp}\right) \le b \tag{2}$$

$$\sum_{p\in P} o_p Q_{jp} \le \sum_{k\in K_j} a_k X_{jk} \qquad j \in J \tag{3}$$

$$\sum_{k\in K_j} X_{jk} \le 1 \qquad j \in J \tag{4}$$

$$X_{jk} \in \{0,1\} \qquad j \in J,\ k \in K_j \tag{5}$$

$$Q_{jp} \ge 0 \qquad j \in J,\ p \in P \tag{6}$$

The objective function (1) minimizes total expected (anticipated) second stage objective function value over the planning horizon. Constraint (2) guarantees that total fixed costs for establishing DCs and holding inventories do not exceed the budget. Constraints (3) require that inventory can be held at a DC only if it is opened, in which case total inventory held cannot not exceed its capacity. Constraints (4) ensure that at most one configuration from set K_j is chosen for DC j. Constraints (5) are the binary constraints for location variables. Finally, constraints (6) are the non-negativity constraints for the quantity of each item held in each DC.

Second Stage (Anticipated Operational Decisions)

A possible anticipation $\mathrm{V}(\mathbf{X},\mathbf{Q},\omega)$ of the effect of prepositioning decisions over daily delivery operations can be obtained using an estimate unit cost of transporting an item from DCs to PODs, instead of actual routing costs. Moreover, as discussed in the previous section, hazard response duration can also be aggregated into its two major phases $\tau = D, SR$. Thus, $\mathrm{V}(\mathbf{X},\mathbf{Q},\omega) = \sum_{h\in \mathrm{H}(\omega)} \sum_{\tau=D,SR} \mathrm{V}^{\tau}(\mathbf{X},\mathbf{Q},h)$, where $\mathrm{V}^{\tau}(\mathbf{X},\mathbf{Q},h)$ is the optimal value of second stage objective function during phase τ of a hazard $h \in \mathrm{H}(\omega)$. Using DC opening decisions in $\mathbf{X}$ the set of available DCs under hazard h is given by $J^h(\mathbf{X})$. Furthermore, each hazard $h \in \mathrm{H}(\omega)$ is characterized by the set of demands $d_{ip}^{h\tau}, i \in I_z, z \in Z^h, p \in P, \tau = D, SR$. During hazard h time to recovery, demand for item $p \in P$ may be satisfied from the following sources:

1- Quantities $Q_{jp}, j \in J^h(\mathbf{X}), p \in P$ prepositioned at opened DCs $j \in J^h(\mathbf{X})$
2- A set of preselected vendors $V_p^h \subset V$
3- A backup source $v = 0$ used as last recourse in case supplies available from DCs and vendors are not sufficient to ensure a timely response.

Hence, the following decision variables are required to formulate the second stage program:

$Y_{pnn'}^{h\tau}$: quantity of item p delivered from origin n (0, v or j) to destination n' (i or j) during phase $\tau = D, SR$ of hazard h.

i) Deployment phase

To capture the high time pressure inherent to the deployment phase, a service-based objective function is used. The intent is to speed up the delivery of each item to demand points by rewarding the proximity of DCs to PODs, using a set of coverage levels. For each POD several coverage levels are defined based on the distance between the POD and the DCs and a reward (penalty) is offered to the nearest (farthest) levels. During the deployment phase, demand for item $p \in P$ may be satisfied with different coverage levels $l \in L_p$. For a multi-hazard h, let

$J_{li}^h(\mathbf{X})$: Set of DCs that can provide coverage level $l \in L_p$ to POD $i \in I^h = \bigcup_{z\in Z^h} I_z$, i.e. set of DCs that are within a distance r_i^l from POD i ($J_i^h(\mathbf{X}) = \cup_l J_{li}^h(\mathbf{X})$).

V_{lip}^h: Set of vendors that can deliver item p to POD i within coverage level l ($V_{ip}^h = \cup_l V_{lip}^h$).

I_j^h: Set of PODs that can be covered from DC j ($I_j^h \subset I^h$).

I_{vp}^h: Set of PODs that can be covered from vendor v for item p ($I_{vp}^h \subset I^h$).

S_{vp}; Maximum quantity of item p that can be provided by vendor v.

Each coverage level l for item p is associated with penalties u_{lp}^J and u_{lp}^V incurred when item p is delivered from a DC or a vendor, respectively. A large penalty u_p^0 is also incurred when demand for item p is satisfied from the backup source. These penalties are proportional to the distance between the network nodes in order to underline the criticality of additional delays to deliver emergency items. In order to encourage deliveries within lower coverage levels and to ensure that demand is satisfied from vendors only when prepositioned supplies are depleted, penalties are specified so that $0 = u_{1p}^J < u_{2p}^J < \cdots < u_{|L_p|p}^J < u_{1p}^V < u_{2p}^V < \cdots < u_{|L_p|p}^V < u_p^0,\ p \in P$. Using this notation, the second stage program for the deployment phase of disaster h is:

$$V^D(\mathbf{X}, \mathbf{Q}, h) = \text{Min} \sum_{i \in I^h} \sum_{p \in P} \left[\sum_{l \in L_p} \left(u_{lp}^J \sum_{j \in J_{li}^h(\mathbf{X})} Y_{pji}^{hD} + u_{lp}^V \sum_{v \in V_{lip}^h} Y_{pvi}^{hD} \right) + u_p^0 Y_{p0i}^{hD} \right] \quad (7)$$

subject to

$$\sum_{i \in I_j^h} Y_{pji}^{hD} \leq Q_{jp} \qquad j \in J^h(\mathbf{X}),\ p \in P \quad (8)$$

$$\sum_{i \in I_{vp}^h} Y_{pvi}^{hD} \leq S_{vp} \qquad v \in V^h,\ p \in P \quad (9)$$

$$\sum_{j \in J_i^h(\mathbf{X})} Y_{pji}^{hD} + \sum_{v \in V_{ip}^h} Y_{pvi}^{hD} + Y_{p0i}^{hD} = d_{ip}^{hD} \qquad i \in I^h, p \in P \quad (10)$$

$$Y_{pji}^{hD}, Y_{pvi}^{hD}, Y_{p0i}^{hD} \geq 0 \qquad j \in J^h(\mathbf{X}), v \in V^h,\ i \in I^h, p \in P \quad (11)$$

Objective function (7) minimizes the total penalty associated to satisfying POD demands within higher coverage levels. It also ensures that demand is satisfied from available vendors only when prepositioned supplies are depleted. In addition, the penalties values structure used in the objective function guarantees that the backup source is used only as a last recourse with a very large penalty. Constraints (8) ensure that prepositioned quantities of items at each available DC are not exceeded. Their slack variables provide the inventory of item p left in DC j at the end of the deployment phase. Constraints (9) guarantee that maximum vendor supply quantities are not exceeded. Constraints (10) ensure that the deployment demand is satisfied, either from the DCs, the vendors or the backup source. Finally, (11) are non-negativity constraints for the deployment decision variables.

ii) Combined sustainment-recovery phases

Recall that during the sustainment-recovery phase, consumable items $p \in P^C$ only need to be shipped to PODs. During this phase, consumable products are mainly shipped from opened DCs, and quantities shipped must be resupplied from the vendors or the backup source. In other

words, during these phases, we must have flow equilibrium at the DCs. Moreover, it is assumed that the shipping capacity of available DCs is sufficient to support daily throughputs. Furthermore, the start of the sustainment-recovery phases marks the end of the chaotic deployment phase and thus the urgent nature of deliveries. In this context, a cost-based objective function is more suitable than a service-based one for these phases. More specifically, the objective for these phases is to minimize total operating costs, which include the procurement of items from the backup source and the vendors, as well as the transportation of these items to the DCs and to the PODs. A unit transportation cost c_{pji} is incurred when an item p is delivered from DC j to POD i. A procurement and transportation cost g_{pvi} is incurred when an item p is delivered directly from vendor v to POD i. Similarly, a cost g_{pvj} is charged when an item p is purchased and transported from source v (vendors and backup) to DC j. The resulting second-stage program for the sustainment-recovery phases under hazard h, is written as follows:

$$V^{SR}(\mathbf{X},\mathbf{Q},h) = \text{Min}\left\{\sum_{p\in P^C}\left(\sum_{i\in I^h}\left[\sum_{j\in J^h(\mathbf{X})} c_{pji}Y_{pji}^{hSR} + \sum_{v\in V^h} g_{pvi}Y_{pvi}^{hSR}\right] + \sum_{j\in J^h(\mathbf{X})}\left[\sum_{v\in V^h} g_{pvj}Y_{pvj}^{hSR} + g_{p0j}Y_{p0j}^{hSR}\right]\right)\right\} \quad (12)$$

subject to

$$\sum_{j\in J^h(\mathbf{X})} Y_{pji}^{hSR} + \sum_{v\in V_p^h} Y_{pvi}^{hSR} = d_{ip}^{hSR} \qquad i\in I^h,\ p\in P^C \quad (13)$$

$$\sum_{\tau=D,SR}\sum_{i\in I^h} Y_{pji}^{h\tau} = \sum_{v\in V_p^h} Y_{pvj}^{hSR} + Y_{p0j}^{hSR} \qquad j\in J^h(\mathbf{X}),\ p\in P^C \quad (14)$$

$$Y_{pji}^{hSR}, Y_{pvi}^{hSR}, Y_{pvj}^{hSR}, Y_{p0j}^{hSR}, Y_{pji}^{hD} \geq 0 \qquad j\in J^h(\mathbf{X}),\ v\in V^h,\ i\in I^h,\ p\in P^C \quad (15)$$

In this model, the objective function (12) minimizes total transportation and procurement costs. Constraints (13) ensure that POD demand of each consumable item is fully satisfied from available DCs and vendors. Constraints(14)[3] ensure that at the end of the recovery period, the prepositioned quantities of consumable items used during the three phases have been resupplied for all DCs. It is assumed that all durable assets are reusable and therefore there is no need to acquire them at the end of the hazard. Finally, constraints (15) are the required non-negativity constraints. It is worth noticing that models (7)-(11) and (12)-(15) are not separable due to constraints set (14).

Integrated Stochastic Programming Formulation

The complete stochastic program to solve is obtained by integrating the previous second-stage deployment and sustainment-recovery models with the first-stage program, for all hazards

[3] This constraint is a transformation of the following inventory accounting relationship:
$Q_{jp} = (Q_{jp} - \sum_{i\in I^h} Y_{pji}^{hD}) + (\sum_{v\in V_p^h} Y_{pvj}^{hSR} + Y_{p0j}^{hSR}) - \sum_{i\in I^h} Y_{pji}^{hSR}$

in all scenarios. To allow adjusting the importance of high coverage versus low operating costs, the objective function is expressed as a weighted sum of these two criteria. The weight associated to the coverage attribute is denoted by $\gamma \in [0,1]$. Denoting the set of all potential disasters by $\mathrm{H} = \cup_{\omega\in\Omega}\mathrm{H}(\omega)$, the program to solve is the following:

$$\text{Min} \sum_{\omega\in\Omega} p(\omega) \sum_{h\in \mathrm{H}(\omega)} \left\{ \begin{array}{c} \gamma \sum_{i\in I^h}\sum_{p\in P}\left[\sum_{l\in L_p}\left(u^J_{lp}\sum_{j\in J^h_{li}} Y^{hD}_{pji} + u^V_{lp}\sum_{v\in V^h_{lip}} Y^{hD}_{pvi}\right) + u^0_p Y^{hD}_{p0i}\right] + \\ (1-\gamma)\sum_{p\in P^C}\left(\sum_{i\in I^h}\left[\sum_{j\in J^h} c_{pji}Y^{hSR}_{pji} + \sum_{v\in V^h} g_{pvi}Y^{hSR}_{pvi}\right] + \sum_{j\in J^h}\left[\sum_{v\in V^h} g_{pvj}Y^{hSR}_{pvj} + g_{p0j}Y^{hSR}_{p0j}\right]\right) \end{array} \right\} \quad (16)$$

subject to

$$\sum_{j\in J}\left(\sum_{k\in K_j} f_{jk}X_{jk} + \sum_{p\in P} e_{jp}Q_{jp}\right) \le b \quad (17)$$

$$\sum_{k\in K_j} X_{jk} \le 1 \qquad j\in J \quad (18)$$

$$\sum_{p\in P} o_p Q_{jp} \le \sum_{k\in K_j} a_k X_{jk} \qquad j\in J \quad (19)$$

$$\sum_{j\in J^h_i} Y^{hD}_{pji} + \sum_{v\in V^h_{ip}} Y^{hD}_{pvi} + Y^{hD}_{p0i} = d^{hD}_{ip} \qquad i\in I^h,\ p\in P,\ h\in \mathrm{H} \quad (20)$$

$$\sum_{j\in J^h} Y^{hSR}_{pji} + \sum_{v\in V^h_p} Y^{hSR}_{pvi} = d^{hSR}_{ip} \qquad i\in I^h, p\in P^C,\ h\in \mathrm{H} \quad (21)$$

$$\sum_{i\in I^h_j} Y^{hD}_{pji} \le Q_{jp} \qquad j\in J^h,\ p\in P,\ h\in \mathrm{H} \quad (22)$$

$$\sum_{i\in I^h_{vp}} Y^{hD}_{pvi} \le S_{vp} \qquad v\in V^h,\ p\in P,\ h\in \mathrm{H} \quad (23)$$

$$\sum_{\tau=D,SR}\sum_{i\in I^h} Y^{h\tau}_{pji} = \sum_{v\in V^h_p} Y^{hSR}_{pvj} + Y^{hSR}_{p0j} \qquad j\in J^h,\ p\in P^C,\ h\in \mathrm{H} \quad (24)$$

$$\sum_{p\in P^c}\sum_{i\in I^h} Y^{hSR}_{pji} \le \mathrm{M}\sum_{k\in K_j} X_{jk} \qquad j\in J^h,\ h\in \mathrm{H} \quad (25)$$

$$X_{jk}\in\{0,1\},\ Q_{jp}\ge 0 \qquad j\in J,\ k\in K_j, p\in P \quad (26)$$

$$Y^{hSR}_{pji}, Y^{hSR}_{pvi} \ge 0 \qquad j\in J^h, v\in V^h, i\in I, p\in P^C,\ h\in \mathrm{H} \quad (27)$$

$$Y^{hD}_{pji}, Y^{hD}_{pvi}, \ge 0 \qquad j\in J^h, v\in V^h,\ i\in I, p\in P,\ h\in \mathrm{H} \quad (28)$$

$$Y^{hD}_{p0i} \ge 0 \qquad i\in I, p\in P^C,\ h\in \mathrm{H} \quad (29)$$

$$Y^{hSR}_{pvj}, Y^{hSR}_{p0j} \ge 0 \qquad j\in J^h, v\in V^h, p\in P^C,\ h\in \mathrm{H} \quad (30)$$

Note that in this formulation, the sets J^h and their subsets are not dependent on **X** as in the second-stage models. This is because the aim of this integrated program is to find the optimal value of (**X**,**Q**) and therefore **X** is not known beforehand. This is also why constraints (26) must

be added to make sure that, at the operational level, DCs are used only if they are opened. The scalar M in this constraint is an arbitrarily large number.

6. Solution Approach

A major challenge in solving the mathematical program formulated in the previous section comes from the cardinality of the set of plausible scenarios Ω. When continuous probability distributions are used (e.g. Normal item demands and exponential hazard inter-arrival times), there is an infinite number of possible scenarios. This difficulty can be overcomed by using the Sample Average Approximation (SAA) method proposed to solve stochastic programs (Shapiro, 2003). In addition, a multicriteria evaluation approach can be used to select the best design among the set of alternative designs produced by the SAA method. The scenario-based solution approach proposed to produce and evaluate alternative designs is summarized in **Figure 4**. It involves three phases: 1) hazards scenarios generation, 2) design generation, and 3) multicriteria evaluation and selection.

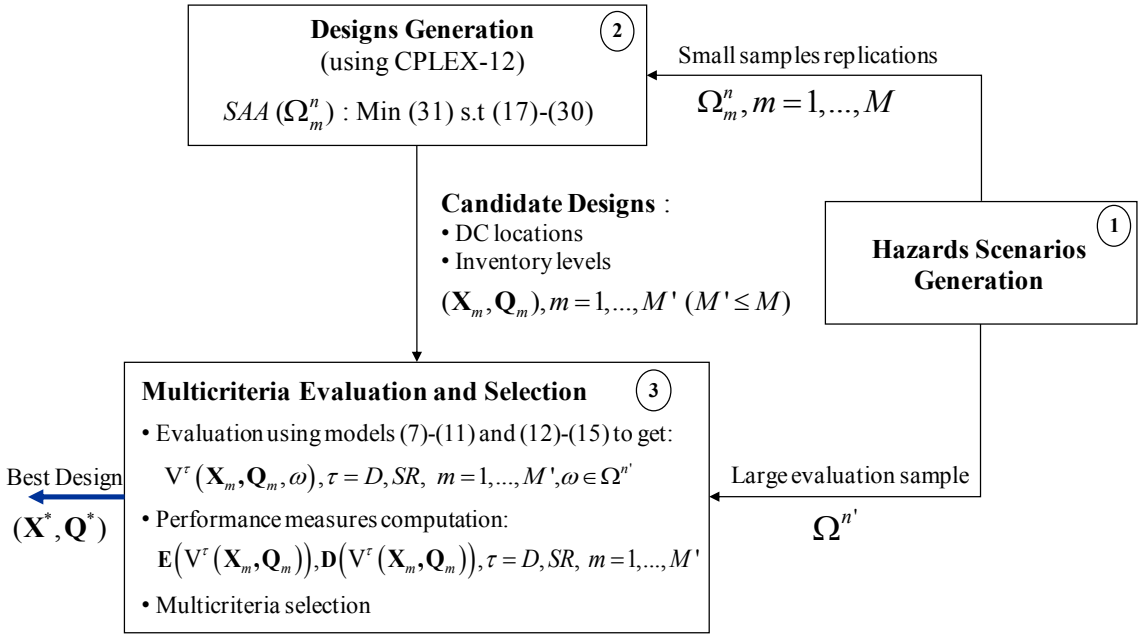

Figure 4- Solution Approach

The scenario generation phase uses the **MonteCarlo** procedure presented in **Figure 3** to provide disaster scenarios to the design generation and evaluation phases. M independent small Monte Carlo samples of n scenarios $\Omega_m^n, m = 1,...,M$, are produced for the design generation phase. A larger sample of scenarios $\Omega^{n'}, n' >> n$ is generated for the design evaluation phase.

The design generation phase uses several samples of scenarios to approximate the proposed mathematical program (16)-(30) by SAA models. This is achieved by replacing the set of scenar-

ios Ω with a sample $\Omega^n \subseteq \Omega$ of n scenarios, and approximating the objective function (16) by (31), to get the following SAA model:

$$\text{Min } \frac{1}{n} \sum_{\omega \in \Omega^n} \sum_{h \in \mathrm{H}(\omega)} \left\{ \begin{array}{c} \gamma \sum_{i \in I^h} \sum_{p \in P} \left[\sum_{l \in L_p} \left(u_{lp}^{J} \sum_{j \in J_{li}^h} Y_{pji}^{hD} + u_{lp}^{V} \sum_{v \in V_{lip}^h} Y_{pvi}^{hD} \right) + u_p^0 Y_{p0i}^{hD} \right] + \\ (1-\gamma) \sum_{p \in P^C} \left(\sum_{i \in I^h} \left[\sum_{j \in J^h} c_{pji} Y_{pji}^{hSR} + \sum_{v \in V^h} g_{pvi} Y_{pvi}^{hSR} \right] + \sum_{j \in J^h} \left[\sum_{v \in V^h} g_{pvj} Y_{pvj}^{hSR} + g_{p0j} Y_{p0j}^{hSR} \right] \right) \end{array} \right\} \quad (31)$$

subject to constraints (17)-(30), with H replaced by $\mathrm{H}^n = \cup_{\omega \in \Omega^n} \mathrm{H}(\omega)$.

As typically done with this approach, the SAA models are used to generate several designs (i.e., prepositioning decisions $(\mathbf{X}, \mathbf{Q})$) using M scenario sample replications. A commercial solver such as CPLEX is then employed to solve the SAA model for the M replications to obtain distinct designs $(\mathbf{X}_m, \mathbf{Q}_m), m = 1, ..., M'$ $(M' \leq M)$.

The design evaluation and selection phase is then required to evaluate these M' alternative designs with a set of performance measures, and to select the best one. Using second stage models (7)-(11) and (12)-(15), each design $(\mathbf{X}_m, \mathbf{Q}_m), m = 1, ..., M'$ is assessed independently for each scenario $\omega \in \Omega^{n'}$, by computing the deployment and sustainment-recovery cost objective function values $\mathrm{V}^\tau(\mathbf{X}_m, \mathbf{Q}_m, \omega), \tau = D, SR$. Using these values a set of performance measures based on sample average and deviation operators can be derived. In our context, for each design $(\mathbf{X}_m, \mathbf{Q}_m)$, the evaluation is based first on the two following expected return measures:

$$\mathbf{E}\left(\mathrm{V}^\tau(\mathbf{X}_m, \mathbf{Q}_m)\right) = \frac{1}{n'} \sum_{\omega \in \Omega^{n'}} \mathrm{V}^\tau(\mathbf{X}_m, \mathbf{Q}_m, \omega), \tau = D, SR \quad (32)$$

A coherent risk measure (Shapiro, 2008) is also used in the evaluation phase. Since downside deviations from mean values are undesirable, each design $(\mathbf{X}_m, \mathbf{Q}_m)$ is assessed with the following mean semi-deviation measures:

$$\mathbf{D}\left(\mathrm{V}^\tau(\mathbf{X}_m, \mathbf{Q}_m)\right) = \frac{1}{n'} \sum_{\omega \in \Omega^{n'}} \max\left[\left(\mathrm{V}^\tau(\mathbf{X}_m, \mathbf{Q}_m, \omega) - \mathbf{E}\left(\mathrm{V}^\tau(\mathbf{X}_m, \mathbf{Q}_m)\right)\right); 0\right], \tau = D, SR \quad (33)$$

Given these evaluations, the selection of the best design among the candidates generated can be done using any multicriteria decision-making method. It is worth noticing that the parameters *n, n'* and *M* need to be carefully adjusted as they greatly impact the solution robustness and quality. Their calibration is based partly on the solvability of the resulting models, and on estimated statistical optimality gaps (Shapiro, 2003).

7. Computational Results

The experiments reported in this section are conducted on a test case inspired from real-world data obtained from the North Carolina Emergency Management Division (NCEM) and the

Federal Emergency Management Agency (FEMA). NCEM actually operates two permanent DCs. In addition, FEMA Incident Support Base at Fort Bragg provides backup assistance in case of major disasters. Our goal is to characterize future disasters threatening the region and identify potential new relief network designs to adequately support emergency operations. In the following, the test case is first described. Then, numerical results are reported and discussed.

7.1 Test Case

The state of North Carolina is partitioned into 101 zones that correspond to counties, each supported by a predetermined set of PODs. The number of PODs per county ranges from 1 to 10 leading to a total of 700 PODs, each with a population varying between 5,000 and 20,000 habitants. Three item families are considered: 1) a typical durable asset, i.e., shelter tents (p = 1) and two types of consumable items, namely, medical kits (p = 2) and a generic item family composed of water and Meals-Ready-to-Eat (MRE) (p = 3). These items can be supplied by 14 potential vendors including the backup source at Fort Bragg. Ten of these vendors are located outside the state and therefore are not prone to the disaster threats under consideration. While the backup source carries all items, eight vendors supply water and MRE, two provide medical kits and three others provide durable assets. **Table 1** shows, for each item, the number of available vendors, their capacity range during the deployment phase (in number of pallets), and their unit price range (in dollars per pallet). The distribution network also includes 10 potential DCs, each with two capacity configuration options (k =1, 2) also shown in **Table 1,** along with their associated fixed opening/usage costs range and inventory holding costs. The latter are expressed as a percentage of items' unit price. The table also provide inbound and outbound transportation costs.

DCs	*k=1* (small)	*k=2* (large)	
Fixed costs ($)	[90K, 148K]	[151K, 232K]	
Storage capacity (pallets)	[770, 1190]	[1210, 1860]	
Inventory holding cost	5%		
Vendors + Backup source	*Durable Assets*	*Medical Kits*	*Water & MRE*
Number	4	3	9
Deployment Capacity (pallet)	[400, 5000]	[700, 1000]	[100, 1600]
Prices ($/pallet)	[1600, 2500]	[1250, 3200]	[1500, 3800]
Transportation			
Inbound unit cost ($)	0.1815 / Pallet-mile		
Outbound unit cost ($)	0.275 / Pallet-mile		
Coverage levels	*Level 1*	*Level 2*	*Level 3*
Maximum Distance (miles)	200	400	800

Table 1-Network Data

Furthermore, it is assumed that a total budget of 1M$ is allocated to preparedness over 3 years. It is also assumed that during the deployment phase, demand at PODs may be satisfied

with 3 different coverage levels: 12, 24 and 48 hours, corresponding to a maximum distance of 200, 400 and 800 miles, respectively. Recall that, for each item p, penalty costs are set so that $0 = u_{1p}^J < u_{2p}^J < u_{3p}^J < u_{1p}^V < u_{2p}^V < u_{3p}^V < u_p^0$ to facilitate delivery within lower coverage levels (ideally level 1), and to ensure that demand is satisfied from vendors only when prepositioned supplies are depleted, the backup source being used as last recourse. In addition, these penalties are set to account for the degree of item's urgency. It is assumed that item 2 (medical kits) is more critical, followed by item 1 and then item 3. Thus, the penalties associated to a coverage level *l* were obtained by multiplying the truckload (TL) transportation rate associated to the level's maximum distance by two coefficients: δ_p^u, the degree of urgency of item *p*, and δ_j^s the priority weight of supply source $j \in J \cup V \cup \{0\}$. The values of δ_p^u were fixed to 1.5, 2 and 1 for items 1, 2 and 3, respectively. The values of δ_j^s were fixed to 1, 5 and 10 for DCs, vendors and the backup source, respectively. The TL transportation rate was estimated to $5.50 per mile, based on trucks capacity.

To estimate disaster stochastic processes, we used historical hazards data spanning the years 1964-2012. In the following, we show how the Monte Carlo procedure in **Figure 3** was used to generate plausible future scenarios. In the derived hazard arrival process, events occur dynamically over a three year planning horizon. The time between two consecutive disasters, estimated at the beginning of the planning horizon, follows an exponential distribution with a historical mean of 434 days. To account for future environmental changes, three equiprobable evolutionary trends $\kappa \in \mathrm{K} = \{1, 2, 3\}$ were used. The first trend is optimistic: fewer disasters are observed compared to the historical trend. The second one is pessimistic and more disasters are observed than in the past. Finally, the third trend corresponds to an "as-is" situation. Under a given evolutionary trend κ, the following linear function is used to derive the mean inter-arrival times in period *t*: $\bar{\lambda}_{t\kappa} = \bar{\lambda}(1 + \hat{\delta}_\kappa t)$, where the slope $\hat{\delta}_\kappa$ is fixed at $-0.00011, 0.00008$ and 0.00003, respectively, for κ = 1, 2 and 3. Additionally, since natural disasters are commonly associated with five levels ranging from very low to very high, the intensity β of an occurring hazard was assumed to follows a discrete Uniform distribution defined on the interval [1, 5].

Since time to recovery θ and severity ρ are random variables correlated to hazard intensity, for a given hazard intensity $\hat{\beta}$, $\theta(\hat{\beta})$ and $\rho(\hat{\beta})$ are random variables with probability distributions specified in **Table 2**. In this table, estimates for the parameters associated to time to recovery are given in days and those associated to severity are given as percentages of impacted zone populations. These estimates are based on historical data and on our discussions with NCEM personnel. Similarly, the deployment phase lasts 3 days, while the recovery duration is estimated to account for 20% of its sustainment counterpart. Collected data are also used to estimate the average daily needs for each product type: a person needs two meals and one gallon of water per day (*p* = 3); a medical kit (*p* = 2) satisfies the weekly demand of 4 persons; and 8 per-

sons use a unit of asset (p = 1). The coefficients of variation for the 3 items are 0.2, 0.2 and 0.1, respectively. Demand for each item is converted to pallet units and a *Log-normal* distribution is used to generate the daily demand for items during the sustainment phase.

Random Variable	β		θ		ρ	
Distribution	*Discrete Uniform*		*Continuous Uniform*		*Continuous Uniform*	
Parameters	Intensity level	Probability	Minimum (days)	Maximum (days)	Minimum (%)	Maximum (%)
	1) Very low	0.35	5	10	0.1	0.3
	2) Low	0.3	5	15	0.2	0.5
	3) Medium	0.2	10	20	0.4	0.7
	4) High	0.1	15	30	0.6	0.9
	5) Very high	0.05	20	45	0.8	1

Table 2: Specifications of Probability Distributions Used in the Monte Carlo Procedure.

Finally, the data available was used to determine the frequency of disasters in counties and of simultaneous hits in nearby counties. These frequencies were then used to estimate centroid zone attenuation probabilities (π_z) and conditional propagation probabilities ($\alpha_{z'|z}$). In our experiments, π_z ranges from 0.003 to 0.015 while $\alpha_{z'|z}$ has an average of 0.36 and a coefficient of variation of 0.7. Additionally, 41% of the probabilities $\alpha_{z'|z}$ are smaller than 0.25 whereas 11% are larger than 0.75. Conversely, estimating DCs and vendors' attenuation probabilities ($\alpha_{j|z(j)}$ and $\alpha_{v|z(v)}$) is challenging due to the lack of historical data. Hence, in our tests for a given facility j (DC or vendor), $\alpha_{j|z(j)}$ equals 0 when $\beta \leq 2$, 0.5 when $\beta = 3$ and 1 when $\beta \geq 4$.

7.2 North Carolina Risk Analysis

This section examines the risk exposure of North Carolina and the extent of relief operations needed in the event of a disaster. **Figure 5** illustrates the distribution of the number of hazards occurring in the state during a 3 year horizon, for a sample of 1,000 scenarios. The scenarios are partitioned into 3 categories according to the number of hits occurring within the horizon: *mild* scenarios if at most one hit is observed, *serious concern* scenarios when the number of hits is between 2 and 4, and *worst case* scenarios otherwise. While **Figure 5** shows a very low probability of worst case scenarios, it also shows a relatively low probability of mild scenarios (i.e., 0.3) compared to its serious concern counterpart (i.e., 0.6). This indicates that the region is undeniably exposed to hazards.

The left plot in **Figure 6** displays the distribution of the number of affected PODs during a scenario and the right plot the distribution of affected population. The figure shows that there is a high probability (i.e., 0.8) of having more than 200 affected PODs, and that more than 400,000 people are involved in 50% of disasters.

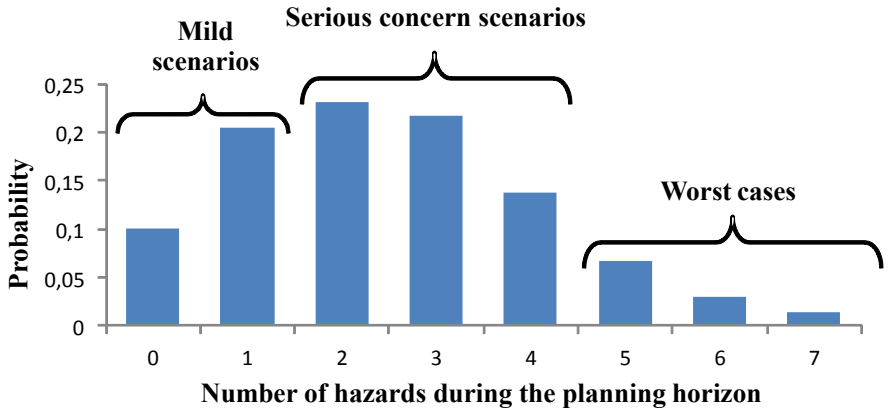

Figure 5- Distribution of the Number of Hazards under a Scenario

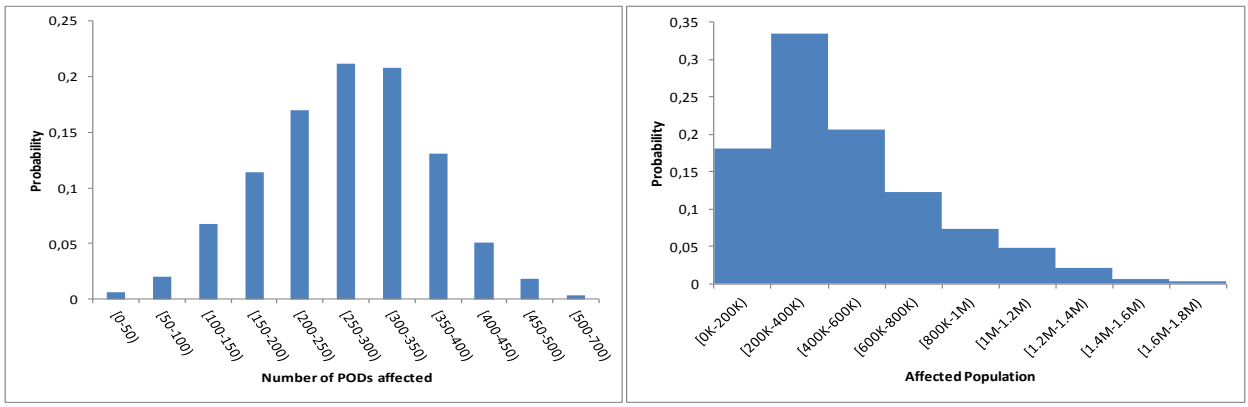

Figure 6- Distributions of the Number of Affected PODs and Population Involved.

Figure 7 illustrates the distribution of water and MRE demand during the deployment phase. It shows that while demand is most likely to range between 4,000 and 6,000 pallets, several severe hazards require up to 30,000 pallets. Similarly, the right plot in **Figure 8** depicts the distribution of daily water and MRE demand during the sustainment-recovery phase. For trucks with a 20 pallets capacity, in 50% of cases more than 100 truckloads must be delivered during a day. The left plot of **Figure 8** displays the distribution of the sustainment-recovery phase duration. Given that the deployment phase lasts 3 days, this figure shows that the time to recovery can reach 6 weeks. It is over 2 weeks in 20% of disasters and below one week in 50% of cases. The latter is due to the low probability of a high intensity hazard in the region (see **Table 2**).

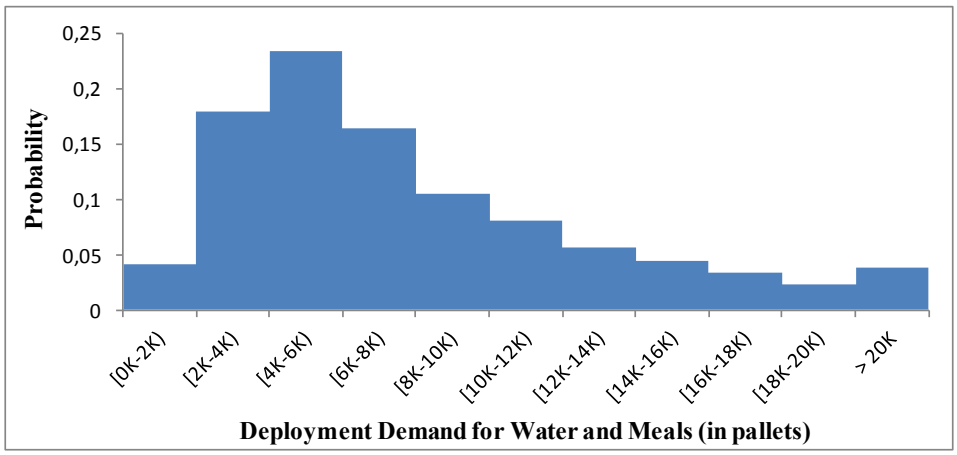

Figure 7- Distribution of Water and MRE Demand during the Deployment Phase

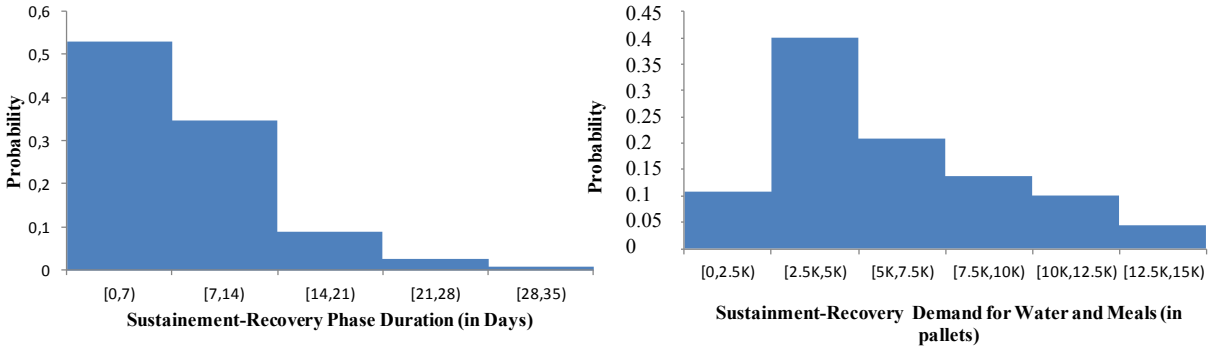

Figure 8-Distributions of Water-MRE Daily Demand and Sustainment-Recovery Duration

These statistics reveal the extent and complexity of relief operations in terms of magnitude of needs, duration and scope. Moreover, the availability of supply sources is an important issue in relief operations. **Figure 9** illustrates the distribution of the number of unavailable DCs/vendors per hazard. It shows a non-negligible probability of a hazard hitting 2 or more DCs/Vendors, which aggravates relief distribution operations.

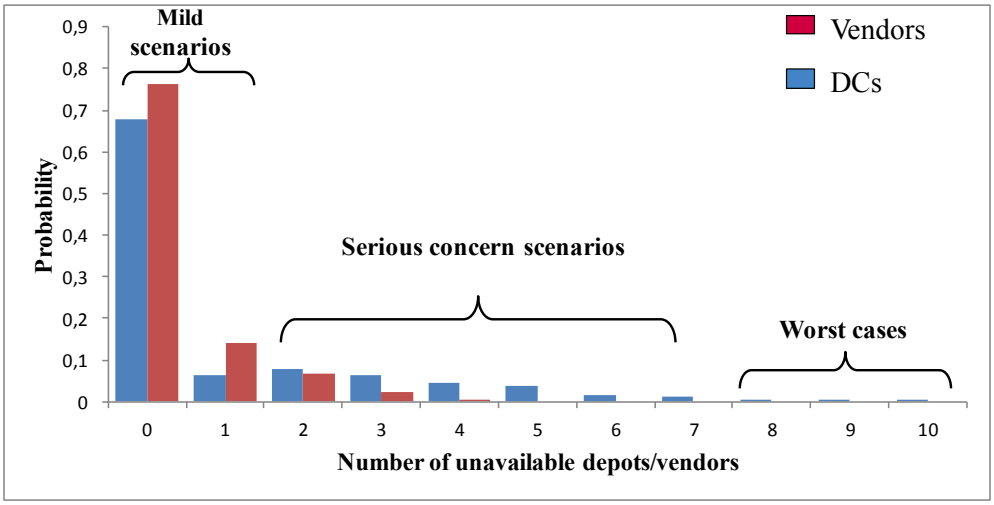

Figure 9- Distribution of the Number of Unavailable Supply Sources

7.3 Network Design Solution Analysis

The aim of this section is to show how to select the best design for the case studied, based on the solution approach (**Figure 4**) described in section 6. This involves the sampling of several small subsets of scenarios, the generation of the corresponding SAA models and their resolution using CPLEX, and the computation of a set of evaluation measures in order to compare them. First, preliminary tests are reported on the SAA models solvability and on the quality of the designs obtained. Next, the set of alternative designs produced using *M* scenario samples are inspected in terms of DC location, capacity and inventory level decisions. To illustrate the key characteristics of the relief network structure obtained, a typical design is analysed in depth. Subsequently, a multi-criteria evaluation of the alternative designs produced is presented, and their performance is discussed. Finally, sensitivity analysis is performed to investigate the impact of varying coverage weights and the prepositioning budget on the solutions produced. The SAA models were solved using OPL-CPLEX 12.3, and the experiments reported were performed on a 64-bit server with a 2.5 GHz Intel XEON processor and 16 GB of RAM.

Calibration Tests

A significant effort has been made to calibrate the size of the scenario samples used in order to guarantee the solvability of the resulting SAA models and the quality of the designs produced. To determine the best value of *n*, sample sizes of 30, 50 and 60 were tested[4], each with 10 replications. Only SAA models with $n = 30$ could be solved to optimality, whereas larger models do not reach the default CPLEX MIP tolerance in a reasonable time. A closer look revealed that, for these models, when approaching optimality, the value of second-stage recourse variables only are modified, and prepositioning decisions remain the same. For this reason a *MIP Relative Tolerance* of 0.005 was used to solve models with $n = 50, 60$.

When observing the variability of the value of objective function (16) between the 10 instances (measured as (max value – min value)/average value), it reaches 66% for $n = 30$, but falls down to about 37% for samples with 50 and 60 scenarios. This could mean that the value of stochastic solutions (Birge and Louveaux, 2011) for our problem is relatively high, which justify the use of a high number of sample replications. The SAA models obtained with $n = 60$ are much more difficult to solve than those obtained with $n = 50$. However, when inspecting the designs obtained with these two sample sizes, we noticed that they are very similar in terms of DCs opening, which was not the case with $n = 30$. For these reasons, a sample size of $n = 50$ scenarios was selected as the best trade-off to use in our experiments. This produces SAA models with 7,052,749 decision variables (including 20 binary variables) and 199,555 constraints. These

[4] Larger scenario samples provide models with more than 10 million decision variables and 250,000 constraints which cannot be solved using CPLEX.

models are solved with OPL-CPLEX 12.3 in 5 hours on average. The number of hazards generated (i.e. the cardinality of H) ranges between [121, 154], which explains the complexity of the second-stage program and the variability of the objective function value.

When generating 10 SAA models (M = 10) and evaluating the resulting designs using a sample of n' = 200 scenarios, a statistical gap (Shapiro, 2003) of 2.57% was obtained, which is relatively low. Remember that objective function (31) of our SAA models includes two criteria, the minimization of a weighted coverage function and the minimization of expected sustainment and recovery costs, and that the former is based on subjective penalty costs set to improve service during the deployment phase. In addition, the relative importance of these two criteria is weighted with the parameter γ (initially set to 0.75) which is also subjectively estimated. Finally, recall that although robustness is an important design criterion, objective function (31) is expressed purely in terms of expected value and does not take dispersion into account explicitly. Given this, the aim of the second phase of our solution approach (**Figure 4**) is to generate a number of good alternative designs, which can subsequently be evaluated using all relevant criteria. This set of potential designs is expended by doing a sensitivity analysis for all subjective parameters. For all these reasons, our experiments were done using the following SAA parameter values: n = 50, M = 10 and n' = 200.

Generated Designs Analysis

The solutions obtained with the 10 SAA models solved with a coverage weight $\gamma = 0.75$ and a budget of 1M$ are summarized in **Table 3**. For each design, the table provides DC opening and configuration decisions, the number of opened DCs, the total inventory level prepositioned in the network, and also the total DCs fixed costs and inventory holding costs incurred. In terms of selected locations, **Table 3** shows that 8 alternative structures were obtained, each involving 5 locations, which is significantly different from the current 2-depot structure. For instance, designs *9* and *10* (similarly, designs *3* and *5*) recommend the same locations and configurations but, the prepositioning of the inventories they propose is slightly different as shown by the inventory costs. On the other hand, although designs *2* and *3* use the same locations, they suggest different configurations (small/large). As can be seen from the inventory costs reported, the inventory levels for the three products prepositioned differ slightly for each design due to the variability within the scenarios sample used. The last column of the table provides statistics on the presence of each DC in the 10 designs produced. This underlines the degree of similarity between the designs obtained and illustrates the importance of *Badin*, *Tarboro* and *Nash* which are always selected. These designs will be examined more thoroughly in the evaluation phase.

	Design 1	*Design 2*	*Design 3*	*Design 4*	*Design 5*	*Design 6*	*Design 7*	*Design 8*	*Design 9*	*Design 10*	
Opening Costs	846 600	846 600	845 800	843 600	845 800	840 600	849 100	843 600	843 800	843 800	
Number of Opened DCs	5	5	5	5	5	5	5	5	5	5	
Inventory Costs	148 700	148 976	148 059	144 761	148 179	146 325	147 541	147 079	148 829	148 654	
Inventory Level	6 260	6 270	6 230	6 090	6 230	6 160	6 210	6 190	6 260	6 260	
DC Location	**Configuration Decisions**										**Presence (%)**
1 **Badin**	2	2	1	2	1	2	2	2	1	1	100%
2 **Tarboro**	2	1	2	1	2	2	2	2	2	2	100%
3 **Nash**	1	2	2	1	2	2	1	2	2	2	100%
4 **Northstar Drive**		1	2	2	2				2	2	60%
5 **Durham**								1			10%
6 **Lincolnton**	1			2		1	1	1			50%
7 **Charlotte**	2								1	1	30%
8 **Leland**						1					10%
9 **Fletcher**		1	1		1		2				40%
10 **Aberdeen**											0%

Table 3- Network Structure Decisions Provided by the Design Generation Phase

To get a better feel of the nature of the designs produced, *Design 1* is illustrated on the North Carolina map in **Figure 7**: the location of the 10 potential DCs is shown and the 5 opened DCs are encircled. **Table 4** provides more details on the solution obtained. Its last row gives total item inventory levels as percentages of expected deployment demand. Note that the two current DC locations used by NCEM are selected in this design but with more capacity. Also, capacity utilizations at opened DCs are at their maximum, which clearly reflects the preference for a deployment from DCs. The item percentages in the last row reflect specified priorities (i.e., assets, then medical kits then water and MRE).

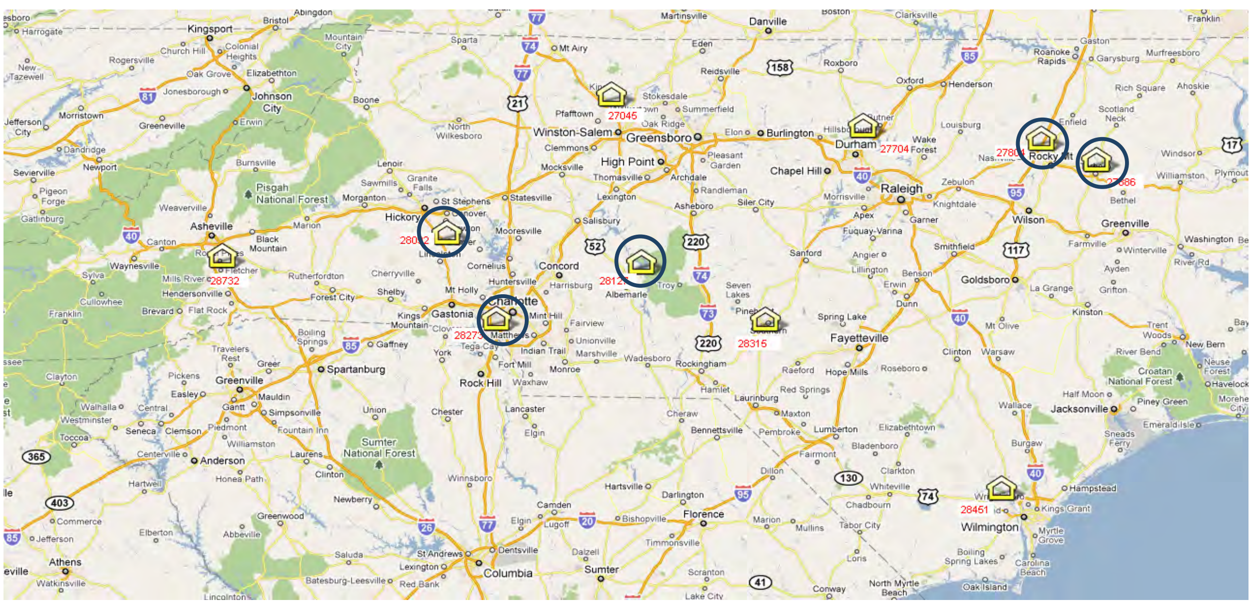

Figure 10- DCs locations for *Design 1* on NC Map

Table 5 presents, for *Design 1*, the proportion of total demand satisfied from DCs, vendors and the backup source for each phase. As expected, during the deployment phase, demand is mostly satisfied from DCs (73%), while backup source and vendors usage proportions depend on the trade-offs between transportation and recourse costs. In addition, our tests indicate that demand is fully fulfilled from DCs only for 41.4% of hazards. This can be in part explained by the

unavailability of some DCs due to disruptions. Conversely, the sustainment-recovery demand is fully satisfied from DCs. This emphasizes the economic benefit of carrying inventories at strategically positioned DCs to take advantage of cheaper delivery directly from these facilities.

		Item inventory levels (in pallets)			
DC Location	*Configuration (square feet)*	*Water-meals*	*Medical kits*	*Assets*	*Capacity usage (%)*
Badin	Large (18 870)	1435	72	3	100%
Tarboro	Large (23 250)	1789	52	19	100%
Nash	Small (9 620)	679	56	35	100%
Lincolnton	Small (9 880)	692	55	43	100%
Charlotte	Large (16 620)	1206	61	63	100%
	Total inventory prepositioned	5801	296	163	
	Expected deployment demand (%)	74,3%	106,9%	117,3%	

Table 4- *Design 1* Solution Characteristics

	Deployment			**Sustainment and Recovery**	
	DCs	Vendors	Backup source	DCs	Vendors
Delivery Average Proportions	73,25%	13,13%	13,62%	100,00%	0 %

Table 5- Delivery Statistics for *Design 1*

Design Solutions Evaluation

This subsection presents the performance comparisons involved in the third phase of the solution approach (**Figure 4**) to evaluate the alternative designs obtained in phase two, and select the best one. Based on our previous analysis of **Table 3** results, it is shown that 10 alternative design structures are distinguished and thus deserves to be evaluated and compared. In what follows, using a large sample of 200 scenarios ($\Omega^{n'}$), all the produced designs (M' = 10) are submitted to the evaluation phase. As indicated in **Figure 4**, at this stage, the evaluation of $V^{\tau}(\mathbf{X}_m, \mathbf{Q}_m, \omega)$, $m = 1,...,M'$, $\omega \in \Omega^{n'}$, $\tau = D, SR$ and the computation of measures (32) and (33) are necessary to compare the performance of these designs.

The repartition of the expected costs between the activities of relief operations are reported in **Table 6** for the two non dominated designs: *Design 9* and *Design 6,* computed using measure (32) for the deployment and the sustainment-recovery phases, respectively. They include expected deployment costs and expected relief operational costs. The later comprise expected costs of supplying DCs and expected costs of delivering to PODs from DCs and vendors. The former express the quality of the responsiveness of the relief service in respect to the coverage level defined. For this criterion, *Design 9* provides the lower deployment cost with 86M$ which means the best relief service. Conversely, as highlighted in the table, the best prepositioning design in terms of economic performance is *Design 6*, with an expected operations costs of 131M$. Most

of this amount comes from the supply costs, which underlines the importance of the upstream level in the network design.

	Operations Costs	Deployment Costs	DC Delivery Costs	Vendor Delivery Costs	Supply Costs	DCs Opening Costs	Inventory Prepositioning Costs
Design 6	131 781 081	87 242 379	1 219 614	2 296 122	128 265 345	840 600	146 325
Design 9	132 192 297	86 639 221	1 227 208	3 805 493	127 159 595	843 800	148 829

Table 6- Non Dominated Designs Expected Performance over a Three Year Horizon

These results are confirmed when comparing, for the 10 designs, the performance measures computed with (32) and (33) for deployment and sustainment-recovery phases. **Table 7** provides the relative deviation in percentage of the performance measures relatively to the best value recorded on each criterion. This table shows also the relative deviation in percentage for three additional compound functions $\mathbf{C}^1$, $\mathbf{C}^2$ and $\mathbf{C}^3$ which are computed as follows: $\mathbf{C}^1$ is the sum of the expected operations costs and the DCs opening and inventory prepositioning costs; $\mathbf{C}^2 = 0.75\mathbf{E}\left(\mathrm{V}^D(.)\right) + 0.25\mathbf{E}\left(\mathrm{V}^{SR}(.)\right)$ is a weighted sum of expected values of reliefs costs and service; and $\mathbf{C}^3 = 0.8\left[\mathbf{E}\left(\mathrm{V}^D(.)\right) + 0.25\mathbf{D}\left(\mathrm{V}^D(.)\right)\right] + 0.2\left[\mathbf{E}\left(\mathrm{V}^{SR}(.)\right) + 0.25\mathbf{D}\left(\mathrm{V}^{SR}(.)\right)\right]$ is a bi-criteria weighted sum of the expectation and deviation measures with a higher weight on the service-based criterion. Note that despite the small percentages of relative deviations, these differences are significant due to the high performance values (**Table 6**).

The results reported, confirm that *Design 9* dominates the other designs on the service-based criterion. When the mean semi-deviation measure of the deployment phase is inspected, *Design 3* could be seen as a good alternative to *Design 9* since it presents a deviation of 0.2% on the expected value and the lowest mean semi-deviation. *Design 9* also dominates other designs when the two compound measures $\mathbf{C}^2$ and $\mathbf{C}^3$ are considered. These two measures combine service and operating costs performance, without and with deviation measure, respectively. This underlines the robustness of this design's network structure to hazards variability. As indicated in **Table 3**, *Design 9* proposes the opening of 5 DCs: *Tarboro*, *Nash* and *Northstar Drive* with large platforms, plus *Badin* and *Charlotte* with small platforms. Total prepositioned supplies include 5,838 pallets of water and MRE, 277 pallets of medical kits and 145 pallets of assets. When compared to the other designs, the delivery performance obtained comes from the high inventory levels at opened DCs. It can also be explained by the positioning of a DC in *Charlotte*, which is rarely the case in the other candidate designs.

On the other hand, when looking at expected relief cost performances, *Design 6* outperforms the other designs. In addition, *Design 6* requires the lowest DC opening and inventory holding costs budget. This is also underlined with measure $\mathbf{C}^1$ that adds the relief operations costs to the budget used, and shows an economy for *Design 6* of more than 0.25% over other designs. In addition to its superior expected costs performance, this design presents a good performance in

terms of the mean semi-deviation in the sustainment-recovery phase (0.08%). However, *Design 6* is ranked only 7th in terms of deployment costs with a 0.7% higher value compared to *Design 9*, which penalises it on the multicriteria evaluation measures. *Design 6* also proposes the opening of 5 DCs: *Badin*, *Tarboro* and *Nash* with large platforms, and *Lincolnton* and *Leland* with small platforms. Total prepositioned supplies include 5,712 pallets of water and MRE, 277 pallets of medical kits and 171 pallets of assets. When compared to the other designs, the main difference comes from a more efficient delivery policy using opened DCs instead of vendors. It is also partially explained by the positioning of a DC at *Leland* , which is never the case in the other designs produced.

	$\mathbf{E}(V^D(.))$	$\mathbf{D}(V^D(.))$	$\mathbf{E}(V^{SR}(.))$	$\mathbf{D}(V^{SR}(.))$	**DCs Opening and Inventory Prepositioning Costs**	$\mathbf{C}^1$	$\mathbf{C}^2$	$\mathbf{C}^3$
Design 1	0,28%	1,65%	0,45%	0,75%	0,85%	0,46%	0,23%	0,27%
Design 2	0,08%	0,67%	0,37%	0,56%	0,88%	0,37%	0,07%	0,05%
Design 3	0,20%	0,00%	0,37%	0,65%	0,70%	0,37%	0,15%	0,08%
Design 4	1,12%	0,11%	0,03%	0,22%	0,15%	0,03%	0,65%	0,60%
Design 5	0,18%	0,13%	0,40%	0,66%	0,71%	0,40%	0,15%	0,08%
Design 6	0,70%	1,03%	0,00%	0,08%	0,00%	0,00%	0,36%	0,37%
Design 7	0,90%	0,79%	0,43%	0,74%	0,98%	0,43%	0,64%	0,61%
Design 8	0,80%	2,06%	0,003%	0,00%	0,38%	0,01%	0,43%	0,51%
Design 9	0,00%	0,99%	0,31%	0,50%	0,58%	0,31%	0,00%	0,00%
Design 10	0,10%	0,86%	0,26%	0,49%	0,56%	0,27%	0,05%	0,05%

Table 7- Comparison of the 10 Designs on the Performance Measures

Design 8 presents the second best alternative when low operating costs are desired whereas *Design 2* presents the second best alternative when a high coverage is desired. Although *Design 1* proposes the lowest expected supply costs, i.e. the most efficient procurement strategy from vendors and backup source, it has globally the worst economic performance. These results, and especially the case of designs *6* and *9*, highlight the conflicting nature of the relief operating costs and the service coverage objectives. Thus, finding a good trade-off between these two criteria is necessary to select the best design. *Design 9* here seems to present the best compromise between cost and service criteria, and it provides a satisfactory performance in terms of robustness.

Sensitivity Analysis

In the following, sensitivity analysis is performed to investigate the impact of varying the prepositioning budget and the coverage weight on the designs produced by the SAA models. Recall that the set of designs presented above was obtained with a 1M$ budget and $\gamma = 0.75$. **Figure 11** illustrates the effects of increasing the budget on the design solution in terms of ex-

pected deployment costs, expected operational costs, number of opened DCs and total inventory level. As observed on the right plot, when the budget rises, the number of opened DCs increases to save on transportation costs. For instance, the number of opened DCs jumps from 5 with 1M$ of budget to 7 with 1.5M$. A maximum of 10 DCs are opened for a budget of 2M$ or higher. An increasing trend is also observed for total inventory level when the budget is bigger which indicates an increase in opened DC capacities and thus a better service. Finally, the decreasing curve of the expected deployment costs shows an improvement in network service performance which reaches a maximum for an allocated budget around 2.5M$. A significant improvement in service performance could thus be obtained by increasing the preparedness budget. However, as shown on the left plot of the figure, this improvement in service performance is negatively correlated to a slight increase in the relief operations costs. This increase is mainly due to the high supply costs involved when the number of opened DCs raises.

Finally, **Figure 12** examines the impact of varying coverage weight on expected operational costs represented by the blue curve, and expected deployment penalty costs depicted by the red curve. The following coverage weights were tested: 0, 0.2, 0.4, 0.6, 0.8 and 1. **Figure 12** indicates that except for the extreme values 0 and 1, the service component of the objective function and its economic counterpart are not very sensitive to the coverage weight. Thus, for other values tested the design structure does not change significantly.

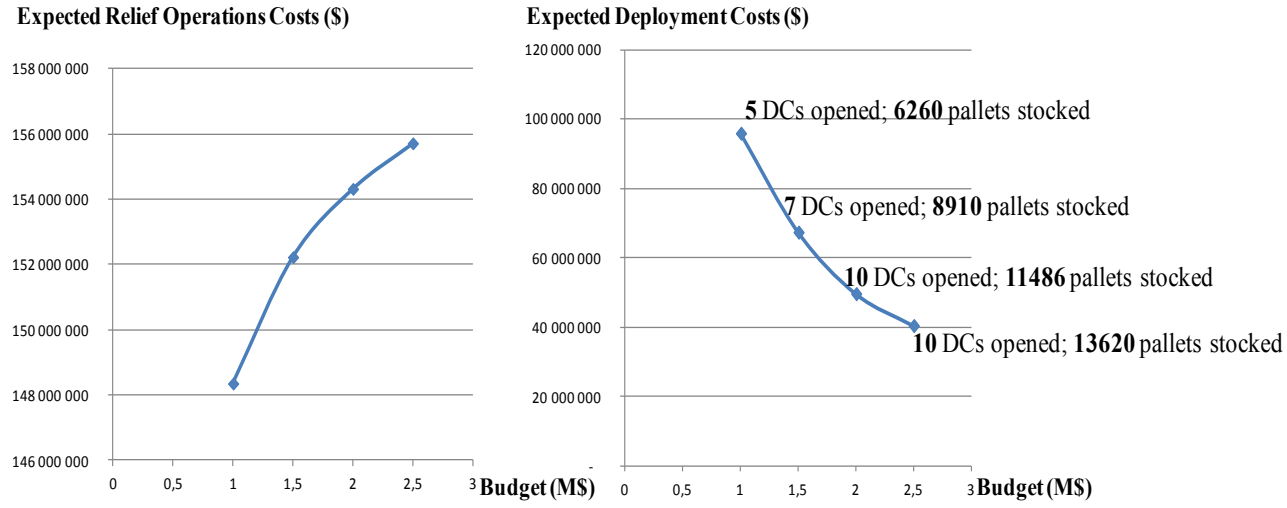

Figure 11- Design Solution Sensitivity to Budget

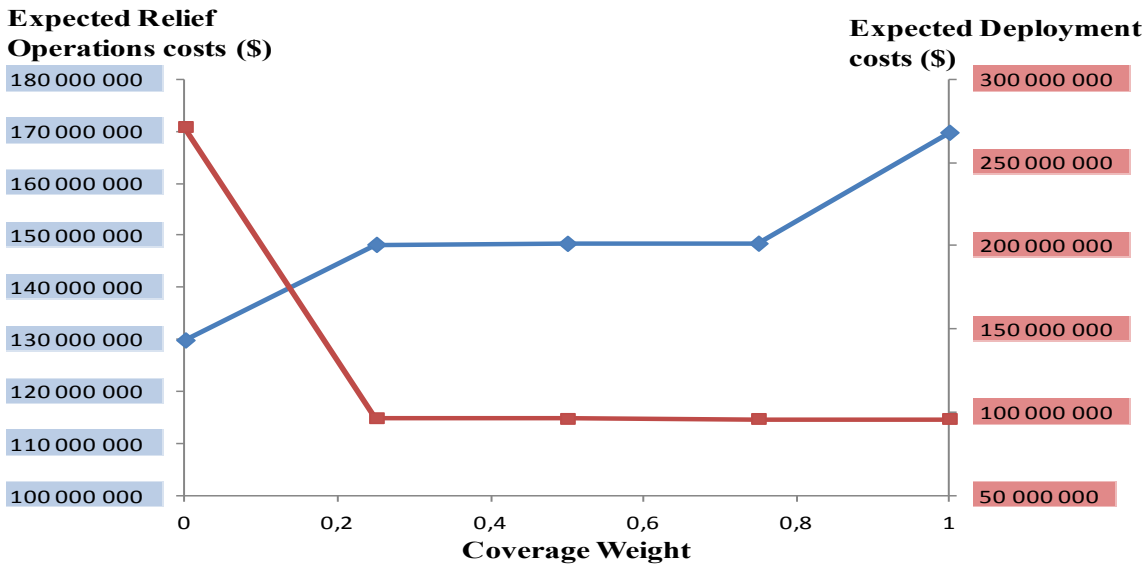

Figure 12- Design Solution Sensitivity to the Coverage Weight

8. Conclusion

This paper presents a scenario based approach for the design of relief networks. The approach proposed involves three phases: scenario generation, design generation and design evaluation. The first phase is a Monte Carlo procedure to generate hazard scenarios over a planning horizon, and it is based on a multi-step disaster modeling approach to specify product demands and relief operations duration. The second phase uses a two-stage stochastic programming model to produce a set of candidate designs. The third phase evaluates and compares candidate designs, using expected value and mean semi-deviation measures based on the performance of the designs for a large sample of scenarios. The approach is assessed using a case study inspired from real-world data provided by the NCEM.

The NCEM uses two DCs to support relief operations in the region. Our objective was to examine the possibility of producing alterative designs to improve relief capabilities. The results obtained show clearly that this objective cannot be attained without deploying a larger number of DCs (5 DCs), and without prepositioning sufficient inventories. Also, our results underline that good service levels can be provided with a relatively small preparedness budget. However, the relief network design case solved included some fictitious, but realistic, data and, before a final decision is reached, more precise data needs to be considered.

The solution approach employed could be improved to tackle larger humanitarian relief problems. Since the solvability of the SAA models is a major concern, the development of heuristic methods and/or sophisticated exact methods need to be pursued in future work. Finally, it would be interesting to apply the risk modeling and the scenario-based solution approach pro-

posed in this paper to humanitarian organisation cases such as the International Federation of Red Cross (IFRC) and the World Food Programme (WFP).

Acknowledgement. Financial support for this work was provided by the National Science Foundation (NSF) through grant number 0927129 (Ichoua). This support is gratefully acknowledged.

References

[1] Akkihal, A.R. (2006). *Inventory pre-positioning for humanitarian operations*, Master's thesis, MIT.

[2] Atlay, N. and W. Green (2006). OR/MS research in disaster operations management. *European Journal of Operational Research*, 175(1):475–493.

[3] Balcik, B. and Beamon, B.M. (2008). Facility location in humanitarian relief. *International Journal of Logistics: Research and Applications* 11(2), 101-121.

[4] Birge, J.R. and F. Louveaux, *Introduction to Stochastic Programming*, Springer (2011).

[5] Campbell A.M. and P.C. Jones (2011). Prepositioning Supplies in preparation for disasters, *European Journal of Operational Research,* 209(2), 156-165.

[6] Chang, M. S, Tseng, Y. L. and Chen, J. W. (2007). A scenario planning approach for the flood emergency logistics preparation problem under uncertainty, *Transportation Research Part E* 43, 737–754.

[7] Daskin, M.S. (1995). *Network and discrete location: Models, algorithms and applications*, Wiley New York.

[8] Daskin M.S, Hesse SM and Revelle CS (1997). α-Reliable p-minimax regret: a new model for strategic facility location modeling. *Location Science* 5(4), 227–246.

[9] Dekle, J., Lavieri, M.S., Martin, E., Emir-Farinas, H., Francis, R.L. (2005). A Florida county locates disaster recovery centers. *Interfaces* 35 (2), 133–139.

[10] Duran, S., Gutierrez, M. A. and Keskinocak, P, 2011, Pre-Positioning of Emergency Items Worldwide for CARE International, *Interfaces* 41(3), 223-237.

[11] Gormez, N. , M. Koksalan, and F. S. Salman, "Locating Disaster Response Facilities in Istanbul", *Journal of the Operational Research Society*, 62:7, 1239-1252, 2011.

[12] Grossi, P. and H. Kunreuther, (2005). *Catastrophe modeling: A new approach to managing risk*. Springer-Verlag, New York.

[13] Guha-Sapir D, Vos F, Below R, with Ponserre S. Annual Disaster Statistical Review 2010: The Numbers and Trends. Brussels: CRED; 2011, from URL: http://www.cred.be/sites/default/files/ADSR_2010.pdf, Accessed January 23, 2012.

[14] Halper, R. and S. Raghavan, (2011). "The Mobile Facility Routing Problem," *Transportation Science*, 45(3), 413-434.

[15] Haimes Y.Y. (2004). *Risk modeling, Assessment, and Management*. Second edition. Wiley..

[16] Iakovou, E, Ip, C. M., Douligeris, C. and Korde, A., (1996). Optimal location and capacity of emergency cleanup equipment for oil spill response, *European Journal of Operational Research* 96(1), 72-80.

[17] Ichoua, S., (2011). Relief Distribution Networks: Design and Operations (Ch. 8). In *Supply Chain Optimization, Design & Management: Advances and Intelligent Methods* (pp. 171-186). IGI Global Hershey, Pennsylvania.

[18] Jia, H., Ordonez, F. and Dessouky, M., (2007). A modeling framework for facility location of medical services for large-scale emergencies, *IIE Transactions* 39 (1), 41-55(15).

[19] Klibi, W and A. Martel, (2012), Scenario-Based Supply Chain Network Risk Modeling, *European Journal of Operational Research*, 223, 644–658.

[20] Lodree, E.J., Taskin, S., (2008a). An insurance risk management framework for disaster relief and supply chain disruption inventory planning. *Journal of the Operational Research Society* 59 (5), 674–684.

[21] Lodree, E.J., Taskin, S., (2008b). Supply chain planning for hurricane response with wind-speed information update. *Computers and Operations Research* 36, 2–15. Special Issue on Disaster Recovery Planning.

[22] Martel A., A. Benmoussa, M. Chouinard, W. Klibi and O. Kettani, (2012). Designing Global Supply Networks for Conflict or Disaster Support: The Case of the Canadian Armed Forces. *Journal of the Operational Research Society*, 65, 1-20.

[23] Mete, H.O. and Z.B.Zabinsky, (2010). Stochastic optimization of medical supply location and distribution in disaster management. *International Journal of Production Economics* (special issue on Disaster Supply Chains) 126 (1), 76–84.

[24] Murali, P., F. Ordonez, and M.M. Dessouky, , (2011). Capacitated facility location with distance dependent coverage under demand uncertainty. Special Issue of Networks & Spatial Economics on Facilities Location. Submitted for publication.

[25] Nolz P.C., F. Semet and K.F. Doerner, (2011)., Risk approaches for delivering disaster relief supplies, *OR Spectrum* 33 (3), 543-569.

[26] Rawls, C.G. and M.A. Turnquist, (2010). Pre-positioning of emergency supplies for disaster response, *Transportation Research Part B* 44, pp. 521–534.

[27] Rawls, C.G. and M.A. Turnquist, (2011). Pre-positioning planning for emergency response with service quality constraints, *OR Spectrum* 33 (3), 481–498.

[28] Rawls, C.G. and M.A. Turnquist, (2012). Pre-positioning and dynamic delivery planning for short-term response following a natural disaster, *Socio-Economic Planning Sciences* 46, 46-54.

[29] Scawthorn, C., Shneider, P.J., Shauer, B.A., (2006). Natural hazards – the multihazard approach. *Natural Hazards Review* 7 (2), 39.

[30] Shapiro A., (2003). *Monte Carlo Sampling Methods*, Chapter 6 in Handbooks in OR. & MS. Vol.10, A. Ruszczynski, A. Shapiro Editors, Elsevier.

[31] Shapiro, A. (2008). Stochastic programming approach to optimization under uncertainty. *Mathematical Programming: Series A* 112, 1, 183-220.

[32] Simpson, N.C., Hancock, P.G. (2009). Fifty years of operational research and emergency response. *Journal of the Operational Research Society*. 60, 126–139.

[33] Snyder, L.V., (2006). Facility location under uncertainty: a review, *IIE Transactions* 38, 537–554.

[34] Snyder LV, MP Scaparra, MS Daskin and RL Church, (2006).Planning for Disruptions in Supply Chain Networks. *Tutorials in Operations Research*, INFORMS: MD.

[35] Tzeng, G.H., Cheng, H.J. and Huang, T.D., (2007). Multi-objective optimal planning for designing relief delivery systems, *Transportation Research Part E* 43, 673–686.

[36] Ukkusuri, S. V. and W.F., Yushimoto, (2008). Location Routing Approach for the Humanitarian Prepositioning Problem, *Journal of Transportation Research Record*, 18-25.

[37] Van Wassenhove, L. N., (2006). Blackett memorial lecture - humanitarian aid logistics: supply chain management in high gear, *Journal of the Operational Research Society* 57(5), 475-489.